

https://dspace.org/

A Three-dimensional Analysis Of The "hunting" Of An Unflanged Railway Wheelpair In Its Motion Along A Straight Track

Boyd, Charles Olivier

2015-01-12
http://hdl.handle.net/10539/16405

Downloaded from a DSpace repository. https://dspace.org/

The difference in the longitudinal displacements of the shaft ends divided by the shaft length gave the angle of yaw of the wheelpair in any individual photograph, while the average displacements of the ends indicated the distance of the centre of mass from the base line. This data was then plotted against time, as shown in Figures 7.3 and 7.4 (using the information that the camera speed was 32 frame/s). New axes were then drawn midway between the limits of the motion, and using these as bases, theoretical sine waves were plotted as a basis of comparison with experimental results. As the graphs show, the difference was so slight that the conclusion could be drawn that both the yawing and the longitudinal displacements were effectively sinusoidal and that as a consequence no coupling existed between the motions. Since the movements could as a consequence of this be regarded as distinct and unconnected, and as the angular movement of the wheelpair was of paramount importance the dicone yoke (the construction of which was described in the previous chapter) was fitted to the rig so as to eliminate the longitudinal movement of the wheelpair. The data relating to the periods of the two movements is listed in Table 7.1.

Table 7.1: PERIODS OF THE LONGITUDINAL AND ANGULAR MOTIONS

	Longitudinal Motion	Angular Motion
No of frames to complete cycle	40	27.5
Period, S	1.25	0.86
Frequency, Hz	0.80	1.16
Frequency, rad/s	5.02	7.29

Before leaving this series of tests, it is worthy of note that tests were run to see whether there was any relationship

between the critical speed at which hunting commenced and the spring constants of the restraining springs. These results, which are summarized in Table .2, showed an increase in the stiffness of the restraining springs brought about a corresponding increase in the critical rail speed; that is, the ratio to the highest spring stiffness to the lowest stiffness equals the ratio of the highest critical speed to the lowest speed.

Table 7.2: TABLE OF CRITICAL SPEEDS AND SPRING CONSTANTS.

Spring Stiffness, KN/m	Critical speed, m/s	Rail Speed, km/h
6.1	6.3	22.7
8.9	6.5	23.4
11.7	6.7	24.1

7.3 SECOND TEST SERIES

When the second series of tests to be discussed in this chapter were performed, the rig had undergone the final modifications which were described in the previous chapter. Whereas in the earlier tests, much of the emphasis in the work done had been placed on procedures aimed at improving the rig performance, these improvements had now been effected and it was functioning in a manner which made it feasible to concentrate on the principal object ot the experimental work; that is, to answer the questions, why and in what manner did the wheelpair oscillate? It was now possible to investigate the relationship between the yawing and tilting movements. The optical measuring system described in the previous chapter showed that these angular movements had the same periodicity (a not too surprising a

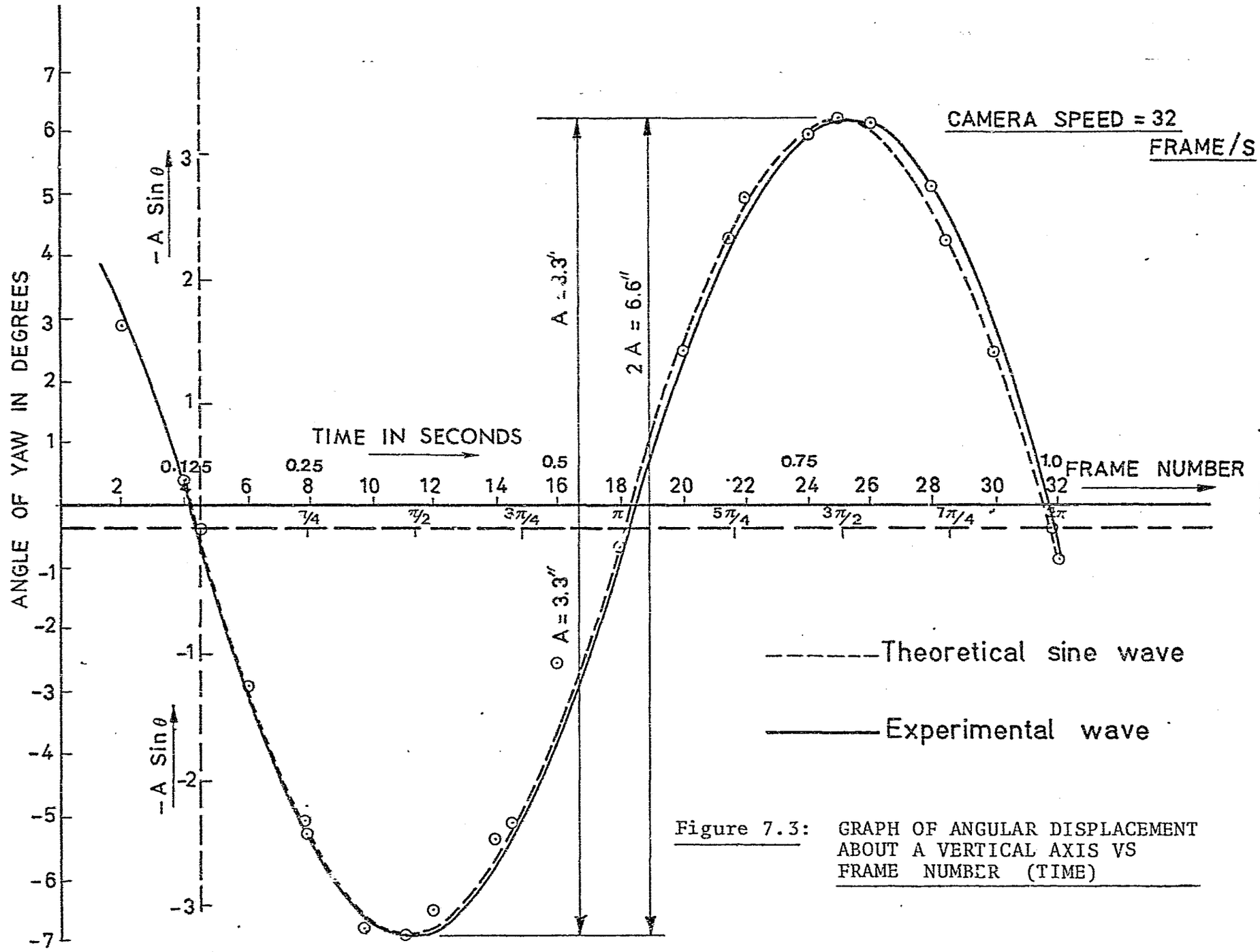

Figure 7.3: GRAPH OF ANGULAR DISPLACEMENT ABOUT A VERTICAL AXIS VS FRAME NUMBER (TIME)

result), and that the phase difference between yawing and tilting being 90°, with the former leading.

An investigation was then made into the nature of the hunting pattern at belt speeds below the critical. As defined earlier, the normal or neutral running position was that position in which the wheelpair neither yawed nor tilted. In this position, the wheelpair has pure rolling motion, as was confirmed by comparing the belt and the wheel spin speeds. The ability of the wheelpair to revert to the pure rolling pattern at belt speeds below the critical was tested by what could be called an 'impulse generator'. A rawhide hammer was so arranged that the head of the hammer was raised to a fixed height above the level of the rails and then released in such a way that it struck the end of the wheelpair shaft in the direction of its major axis of symmetry. (The hammer blow intensity was the same, since the distance through which the hammer head fell was constant.) It was observed that the effect of the hammer blow was to push the wheelpair away from the neutral position, but that after hunting had occurred over several cycles, it would revert to rolling in the neutral position. It was, of course, necessary to take care that once the hammer blow had been struck, the subsequent movement of the wheelpair was not interfered with. A stop watch was started at the instant of impact and stopped when the oscillations ceased so that the period of oscillation could be found. When the wheel spin speed exceeded 4.68 Hz (or 29.41 rad/s), oscillatory motion persisted; it would also start without outside prompting when this wheel spin speed was exceeded. The data recorded during these transient response tests is listed in Table 7.3 and plotted in Figure 7.5.

The disparity between the actual wheelpair spin speed (as

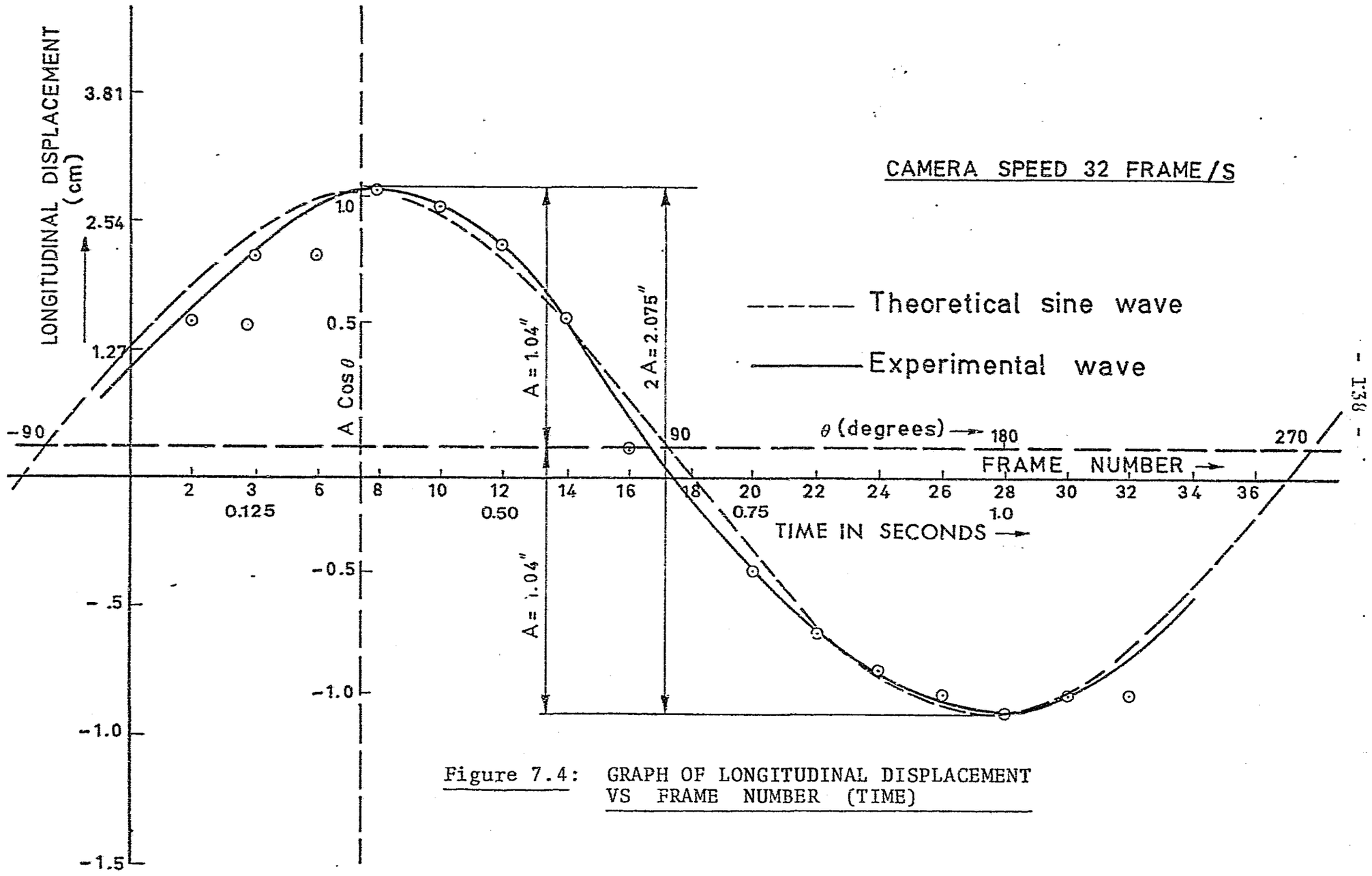

Figure 7.4: GRAPH OF LONGITUDINAL DISPLACEMENT VS FRAME NUMBER (TIME)

determined by a General Electric Strobotac) and the theoretical spin speed was investigated for belt speeds above the critical. The theoretical spin speed was found by

Table 7.3: TRANSIENT RESPONSE TESTS

Wheelpair spin speed, n			Number of Cycles Completed	Frequency of Oscillation, Hz
r/s	rad/s	r/min		
3.40	21.36	204.0	2	1.25
3.78	23.75	226.8	3	1.3
4.10	25.76	246.0	5	1.2
4.42	27.77	265.2	12	1.26
4.53	28.46	271.8	21	1.23

multiplying the driving pulley spin (measured by means of a Smith's mechanical tachometer) by the ratio of the driving pulley radius to the wheelpair running tread radius. The resulting information is given in Table 7.4.

Table 7.4: SLIP AS A FUNCTION OF WHEELPAIR SPIN SPEED

Rail Speed		Hunting Frequency,	Measured Wheelpair spin speed,	Calculated Wheelpair Spin speed,	Slip Speed,	% Slip
m/s	m/min	Hz	r/mm	r/min	r/min	
2.474	148.4	1.233	281.0	281.2	0.2	0.068
2.628	157.7	1.217	299.0	299.4	0.4	0.133
2.783	167.0	1.217	315.0	316.4	1.4	0.44
2.938	176.3	1.233	333.0	334.0	1.0	0.30
3.092	185.5	1.233	349.0	351.5	2.5	0.71
3.278	196.7	1.233	370.0	372.6	2.6	0.69

The information listed in Table 7.4 has been plotted in

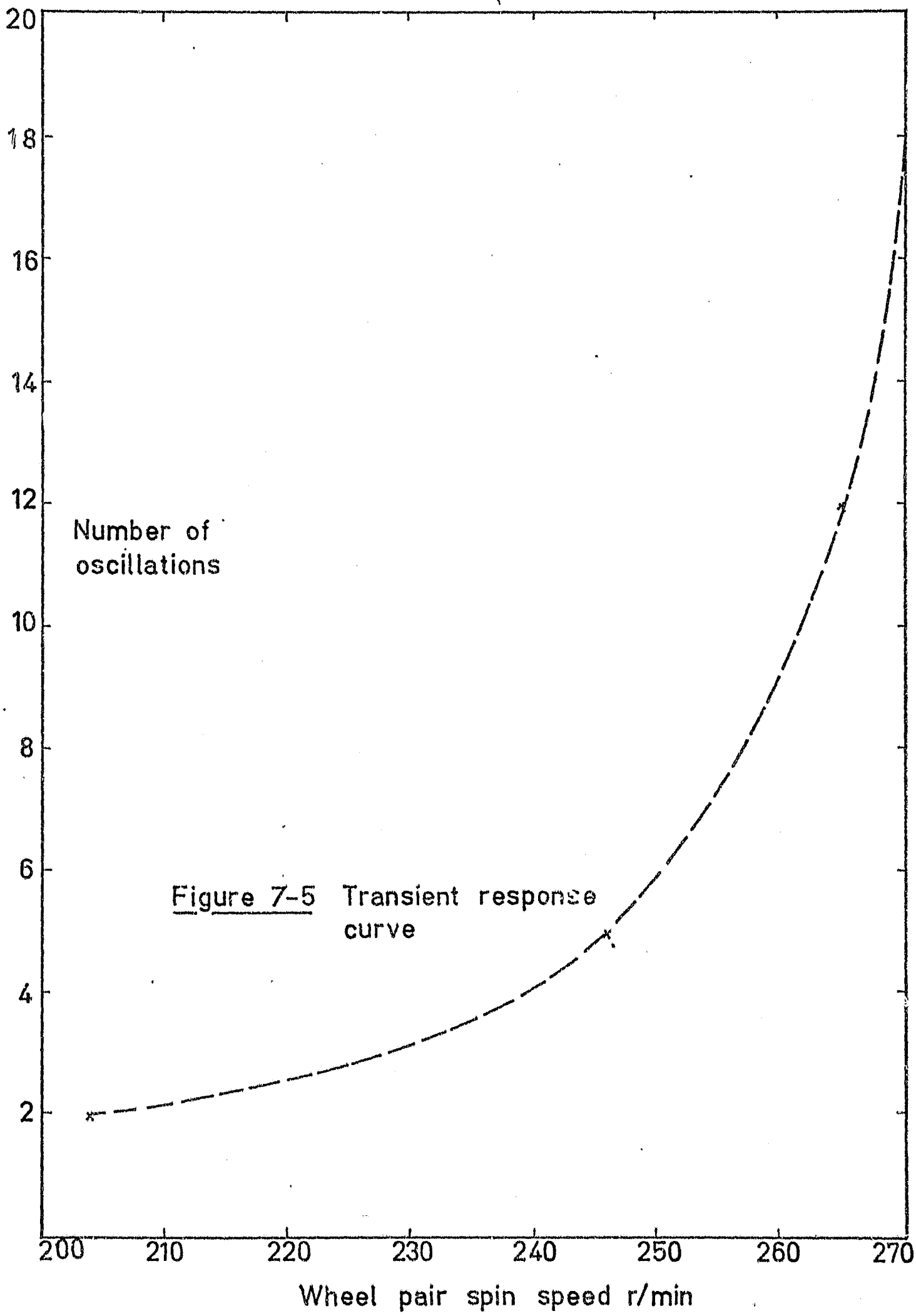

Figure 7-5 Transient response curve

Figure 7.6. This shows that the percentage slip is linearly proportioned to the rail speed while the curve of the slip speed indicates some falling off of the spin speed at higher rail speeds. The cause for this could be a change in the friction characteristic.

Table 7.5 shows the amplitudes of the yawing and tilting motions at various belt speeds.

Table 7.5: RELATIONSHIP BETWEEN THE AMPLITUDES OF THE YAWING AND TILTING MOVEMENTS AT VARIOUS RAIL SPEEDS

Rail Speed,		Wheelpair Spin Speed		Oscillatory Frequency,	Amplitude of yaw,	Amplitude of Tilt,	Ratio Yaw:
m/s	m/min	r/s	r/min	Hz	Degrees	Degrees	Tilt
2.47	148	4.68	280.8	1.23	1.5	0.30	5.00:1
2.63	158	4.97	298.2	1.22	2.0	0.50	4.00:1
2.78	167	5.25	315.0	1.22	2.3	0.60	3.83:1
2.94	176	5.55	333.0	1.23	2.7	0.75	3.33:1
3.09	186	5.82	349.0	1.23	3.0	0.90	3.33:1

Figure 7.7 shows that over the range of speeds tested there is a linear relationship between belt speed and the amplitudes of the yawing and tilting motions. The ratio of the amplitudes of yaw to tilt is for the most part linear and shows a decreasing tendency. The range of speed in the table is relatively limited, with the highest speed being 33% higher than the lowest speed. At higher speeds, the increase in amplitudes slowed down and the motion became stable.

7.4 THIRD TEST SERIES

In the previous test runs, the period of the oscillatory motion had been measured by timing a given number of cycles

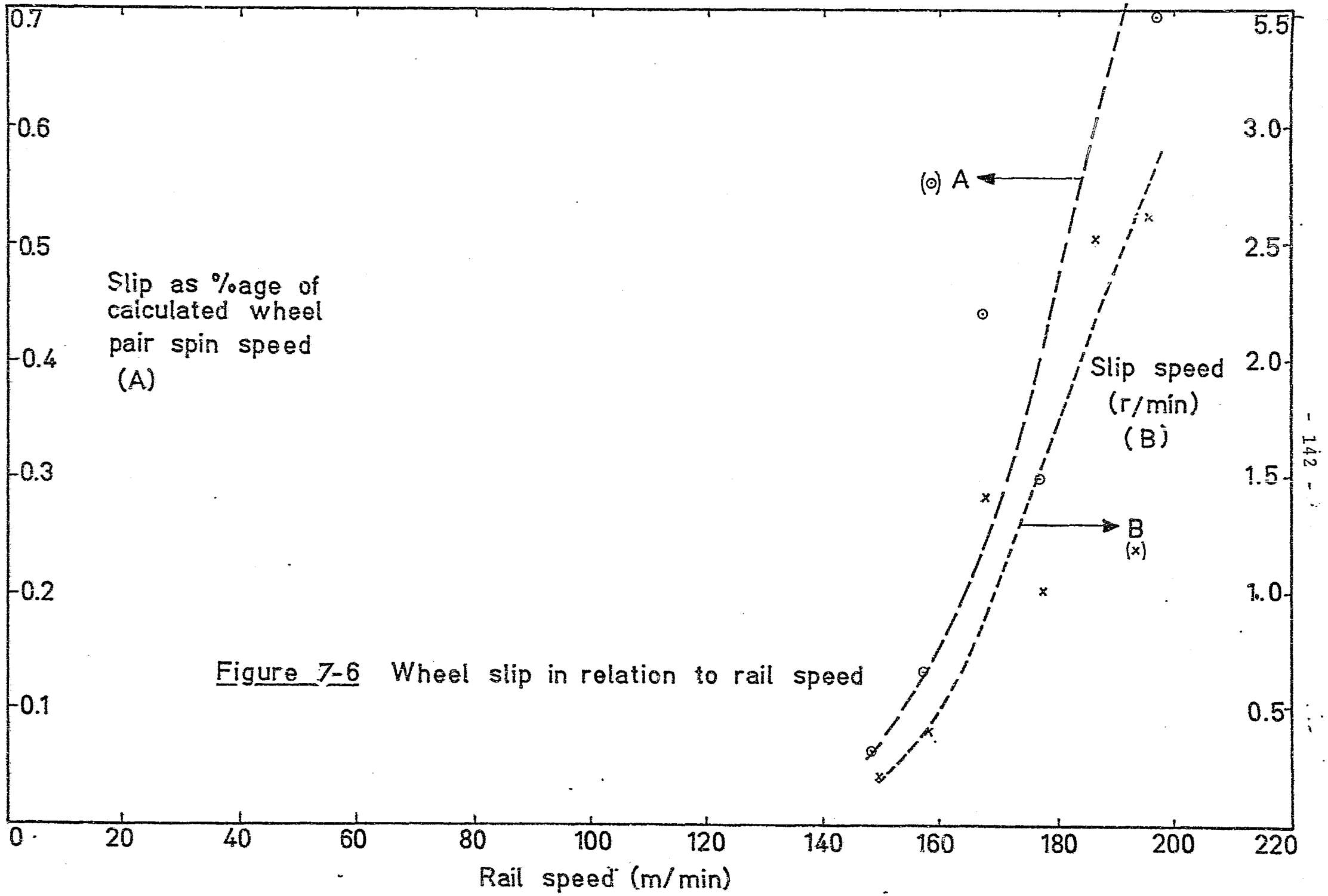

Figure 7-6 Wheel slip in relation to rail speed

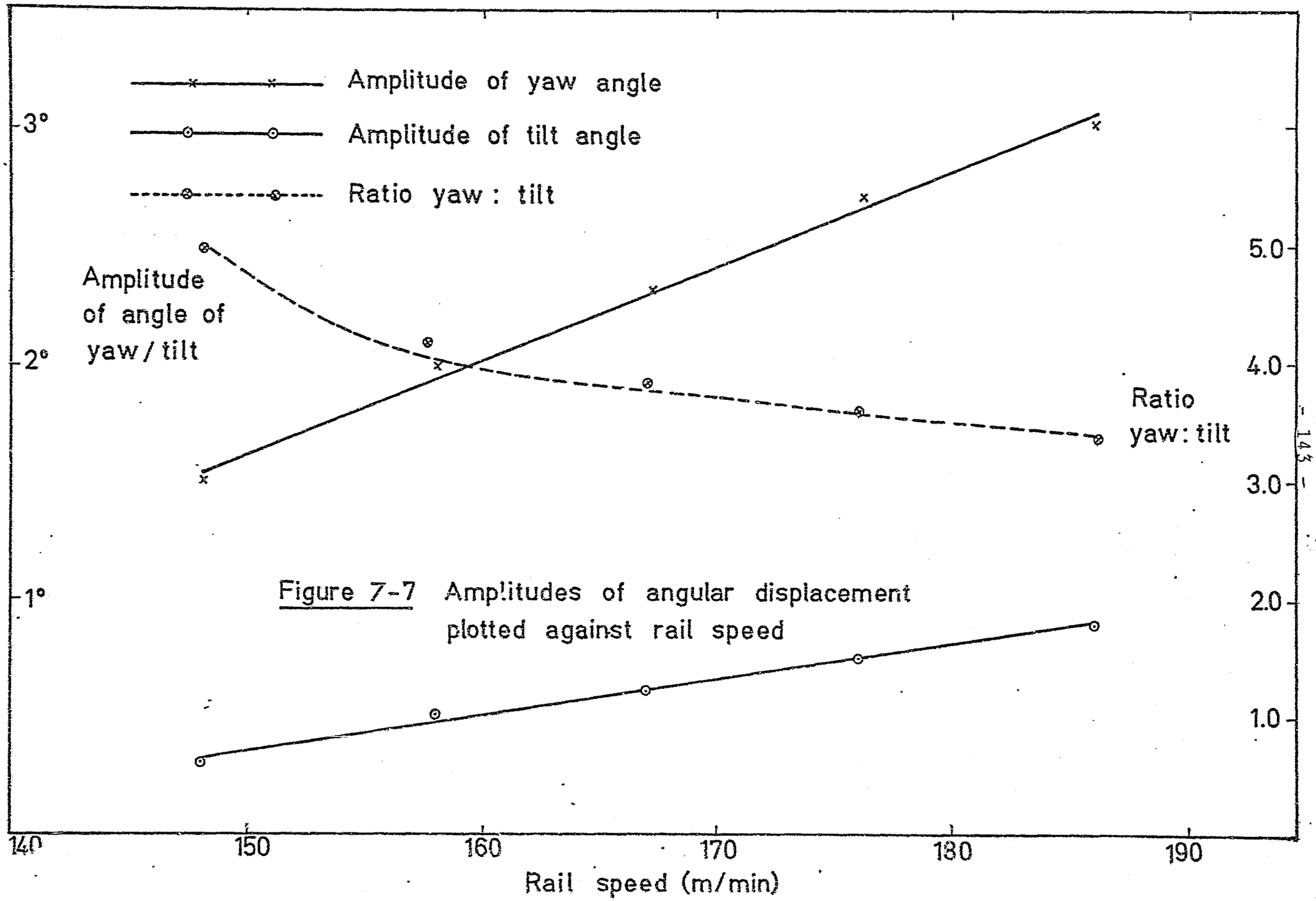

Figure 7-7 Amplitudes of angular displacement plotted against rail speed

with a stopwatch. It was then decided to investigate methods for determining the oscillatory motion frequency more accurately. At first, a Griffin Digital Centisecond Timer fitted with a light source was used where the light beam was reflected off a mirror fixed to the side of the dicone yoke into the photodiode which was part of the Griffin equipment. Because the light source was powered off the AC mains, there was a cyclical variation in brightness and in addition, it was found that the cut-off of the beam as the yoke turned was not sharp enough to trigger the photo diode. The replacement of the power source with a 6 V battery and the addition of a cap with a slit on the light source gave no better results. An argon jet light source, with a built-in adjustable slit powered from a 12 V battery, was then successfully used. The slit of light was focussed through a Leitz Wetzler Milar lens, with a focal length of 10 cm, off the mirror into the photo-
de, which in turn was connected to a Watanabe Multicor-
A recording of the wave form is shown in Figure 6.8.
aks were recorded for each cycle as the dicone yoke
forwards and then back again.)

The wave form recordings gave the frequency of the oscillations in these tests as 1,8 Hz (or 11.3 rad/s). Readings were taken over a range of wheel speeds from 200 r/min to 500 r/min but no change in the frequency of the oscillatory patterns was found over this range. The device for measuring the amplitudes of the angular movement was not used in this series of tests since the brass bearing imposed a load on the wheelpair which had not been allowed for in the theory, but as far as it was possible to observe, the amplitude of the motion did not increase at the higher speeds.

7.5 EXPERIMENTAL PARAMETER DATA

The moments of inertia of the wheelpair which were required to test the validity of the theoretical analysis were determined experimentally by arranging that the wheelpair was swung as a pendulum, first about the principal axis of symmetry (which coincided with the direction of the wheelpair shaft) and then about the principal axis normal to the wheelpair shaft. The relevant moments of inertia were then calculated from the periods of the swings. This and other relevant data for the wheelpair is tabulated in Appendix A1.

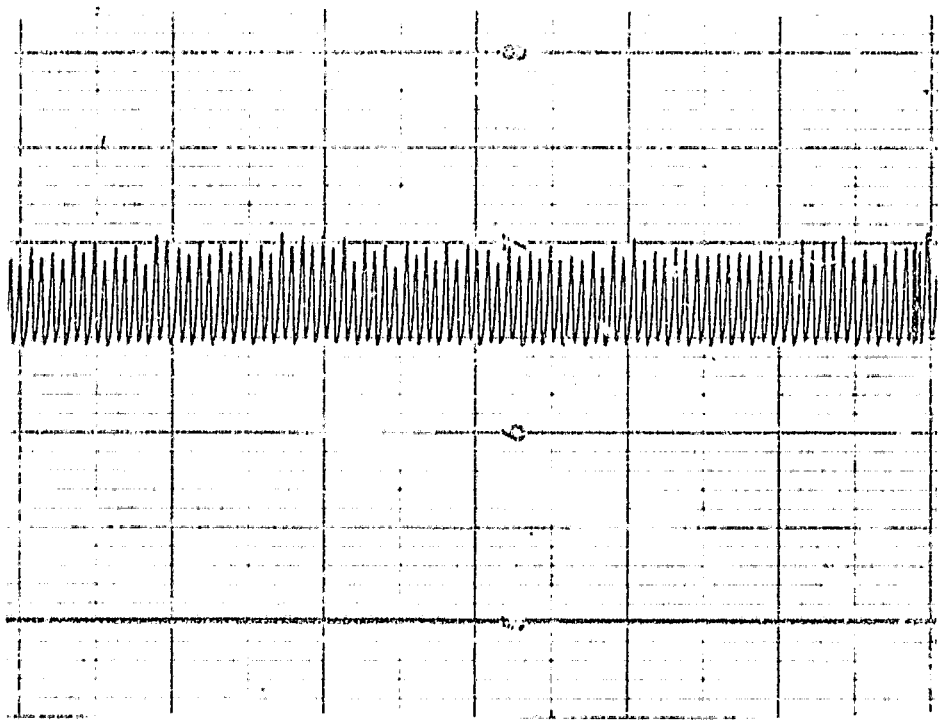

Figure 7.8: WAVE FORM OF FREQUENCY RESPONSE (Paper speed: 0.3 m/min)

CHAPTER 8

A DISCUSSION AND COMPARISON OF THE THEORETICAL AND EXPERIMENTAL RESEARCH

8.1 INTRODUCTORY COMMENTS

The problem of railway hunting has been examined both theoretically and experimentally and, at this point, it is necessary to consider how the two approaches complement each other. For the comparison between the two to be effective, the basis of the comparison must be identified. Essentially, this investigation of the oscillatory behaviour of the wheelpair as it travels along two parallel straight rails (represented as an idealisation as two parallel lines) is viewed as an enquiry into the dynamic behaviour of a rigid body which has a given symmetry about its principal axis and which is constrained to move in a particular manner in three-dimensional space.

The necessity to relate theoretical deductions to experimental performance is illustrated by the following comment of Wickens' [8, page 5] ;

> As the inertia forces increase with speed, eventually they dominate the motion and the system is unstable. It follows that there is a critical speed above which the amplitude of small oscillations grows exponentially and below which small oscillations decay.

Presumably, Wickens believed that the experimental work done at Derby confirmed this prediction. However, as explained at the end of chapter 3, the experimental rig used here has the advantage that it has been possible to observe how the body

(that is, a wheelpair) behaves when no restriction is placed on the amount of yaw and/or tilt it experiences at various rail speeds. There was no evidence whatsoever of an exponential growth in the amplitude of oscillation above the critical speed or of decaying amplitudes below the critical speed. Either the wheelpair rolls in the central or neutral position, or it oscillates with sinusoidal harmonic motion across the rails. Furthermore, this oscillatory motion starts with a finite amplitude; that is, it neither starts from zero nor does it grow exponentially as predicted by Wickens. His view of the critical speed is not confirmed in this work. Here it is believed that as the rail speed is increased, the critical speed is that at which the type of motion changes from one form into another, where the latter movement can be determined theoretically. Since at the instant at which the change occurs, the forces used in the theoretical analysis are not available, it is not clear why and how the break-away occurs.

It is strange but true that despite intensive research, the dynamic behaviour of bodies moving in three-dimensional space is still baffling. Some of the difficulties are commented on by Kharlamov [41] in a recent paper:

> In the solution of an applied problem dealing with a rigid body, the total information about its motion is not always necessary. But if such a problem is considered as an aspect of theoretical mechanics one naturally desires to get a most complete idea of all the peculiarities of the body motion. Poinsot, highly estimating the results of d'Alambert, Euler, Lagrange mentioned however that in all of these researches there was nothing except calculations and that a visual imagination of a motion could not be reached. At best, one could define as a result of a lot of work the position of the body at a given moment of time, but one could not see how the body had come to such a position. We'd like, Poinsot wrote, to have a full imagination of all the stages of motion and to observe the body during all the time of its rotation. If

> such imagination is received, we shall consider, after Poinsot, that the problem of the dynamics of the rigid body has got a complete solution. The bright example of a complete solution is the famous geometrical description which Poinsot gave to a free motion of a body by representing it as a rolling of the ellipsoid of inertia on a rough immovable plane. For a long time this result has been a singular example of a complete solution.
>
> During the last century and at the beginning of the present one several exact solutions in the dynamics of a rigid body were found. Under certain conditions restricting the parameters of the body the considered problem usually was reduced to quadratures and sometimes the possibility of obtaining the dependences of Euler angles on time was shown. To state any conclusions on the character of motion based on those quite complicated dependences seems almost impossible. This fact gave rise to a certain scepticism in the estimation of such mechanical results. These investigations are only of mathematical interest - one can come across the point of view in the researches devoted to the dynamics of a rigid body.

It is unlikely that a complete and definitive explanation of the causes of railway hunting would ever be forthcoming within the compass of a single work such as this. All that can be put forward are suggestions as to how it is believed the oscillatory behaviour is caused, to propose a feasible theory and to devise experimental methods which make observation of the motion possible. However, it must be made clear that whereas other workers - as the quotation from Wickens given earlier in this section shows - are of the opinion that the dynamic behaviour of the wheelpair is dominated by inertia forces, it is now believed that the gravitational potential energy aspect is no less important and that this, in turn, makes it unlikely that the oscillatory motion is in any way determined by linearised differential equations.

8.2 THE PROBLEM OF FREQUENCY SUPPRESSION

If the oscillatory behaviour of the wheelpair were explicable in terms of linearised differential equations, then according to this theoretical approach, the system would operate with two natural frequencies. If the system were oscillating freely, the motion would be a vectorial combination of each

frequency. The effects of only one frequency can be observed experimentally and it is then necessary to explain why the other frequency has been suppressed. Elsewhere, it is noted that the interpretation of the theoretical results could follow a particular pattern and an attempt will now be made to further explain one's understanding of the arguments used.

For a system which has two degrees of freedom, the substitution of one of the frequencies derived from the characteristic or frequency equation (the 'eigen-values') into the equations of motion would produce the ratio for that frequency of the amplitude of the two generalised coordinates (the 'modal ratio' or 'mode'). In the railway hunting situation, this school of thought asserts that the physical coupling within the system is such that at either of the frequencies, one or other of the coordinates is dominant, that is, each of the two modes for any spin speed contains either mostly yaw or mostly tilt components. The lower of the frequencies produces the tilt mode and the higher frequency is responsible for the yaw mode. A confusing complication is that reference is made to self-excited systems, which as far as one is aware, do not occur in systems governed by linear differential equations.

Whatever the merit or otherwise of this argument, the fact remains that the experimental behaviour of the wheelpair showed that yaw and tilt were always present and that it was not a case of 'mostly yaw' or 'mostly tilt'. This lack of agreement between such theoretical predictions and practical experience would suggest that the assumption that hunting is adequately accounted for by linear differential equations requires to be reviewed; however, instead of reaching such a conclusion, it has been suggested that any results obtained should be tailored to a procrustian solution dictated by linear theory.

Obviously, any explanation of how the oscillatory behaviour takes place needs to take into account the physical facts observed during the experimental runs. The previous section referred to the fact that the growth in amplitude did not conform to linear theory, this section refers to the fact that only one experimental frequency can be observed and lastly, there is the fact that there is a constant phase difference of 90° between the yawing and the tilting movements. An explanation for the latter manifestation is offered later in this chapter but it would seem inescapable to conclude that the motion which has been observed is that of an unstable focus which then approaches a limit cycle and that, in turn, it is governed by non-linear differential equations.

8.3 ADHESION BETWEEN THE WHEEL AND THE RAIL

There is somewhat of a dichotomy in the railway literature relating to the nature of the contact between the wheel and the rail which appears to have escaped notice until now. The quotations made so far have been concerned with railway hunting, yet there is another aspect of the rail-wheel contact which has been the concern of a different group of engineers, namely, the need for the wheel to adhere to the rail. It is an aspect which goes back to the beginnings of railway operation; thus, Francis [44] points out:

> For years was the fallacy established in men's minds as fixedly as an article of faith, that the locomotive could not draw heavy loads; that the adhesion of the smooth wheels of the carriage to the smooth rails of the iron must be so slight, that the wheels would move round, the carriage would not move with them. There was no doubt of this in the minds of scientific persons. It had been said by the pundit, it was believed by the scholar. Men published treatises, formed plans, made new discoveries, argued, wrote, pleaded, and finally took out papers to overcome a difficulty which had no existence save in their own minds.

As Collins and Pritchard [45] state:

> The importance of wheel/rail adhesion to the railways needs no emphasis; all traction and breaking forces are in the end limited by the available friction between wheel and rail. Possibly the most troublesome aspect is that adhesion varies in such an unpredictable manner.

The latter authors are concerned with traction and braking but if adhesion is important in these aspects, it must play an equally important part in the ordinary rolling of the wheelpair. It is here that one suspects that insufficient emphasis has been placed on investigating the causes of railway hunting. It is a reasonable deduction that as long as the adherence between the wheel and the rail is adequate, it is possible for the wheel to have pure rolling motion over the rail. This condition is remarkably persistent, as demonstrated by the transient response on the test rig which was described in section 7.3. Once the rail speed had exceeded a certain minimum value, adequate adherence between the wheel and the rail was no longer possible, gross sliding occurred and the hunting pattern of behaviour became apparent.

There are thus two distinct forms of behaviour and it is important that this should be recognised. The theory of creep is helpful in showing the manner whereby adhesion is lost. During an extraordinarily brief transitory period, there is a swift rise in the inertial forces which can no longer be held in check by the adhesion provided by the locked region. As a consequence (since the adherence between the wheel and the rail no longer exists) pure rolling ceases and hunting sets in.

8.4 DISPLACEMENT OF THE CENTRE OF MASS OF THE WHEELPAIR AS IT YAWS AND/OR TILTS

8.4.1 INTRODUCTION

Doubt has been expressed above as to whether any attempt to linearise the equations of motion would prove fruitful in substantiating, on the basis of the experimental results which

have been obtained, the theoretical linearised equations of motion presented. Nevertheless, some of the deductions which can be drawn from the general theoretical analysis are directly useful in that they serve to explain particular aspects of the dynamic behaviour of the wheelpair (such as, for example, the refusal of the wheelpair with a taper angle of 30° to hunt). It is hoped that by expanding of such deductions, sufficient grounds will be provided for substantiating the theoretical analysis.

8.4.2 Lateral displacement of the centre of mass of the wheelpair as it yaws and/or tilts

Certain relationships were derived in Section 5.4.4 to express the position of the centre of mass of the wheelpair as a function in which the angle of yaw (ϕ) and the angle of tilt (θ) were the variables. The lateral displacement of the centre of mass was shown there to be given by

$$b\,Cosec 2\alpha\, Sin 2\theta - R\,Cos\phi\, Sin\theta$$

For small yaw angles (that is, $\phi \to 0$), $Cos\phi \to 1$, so that it is not surprising that yawing (which in effect merely causes the wheelpair to settle more deeply between the rails) should be shown in calculating the lateral displacements for various angles of ϕ and θ to have practially no effect on such displacements. If $Cos\,\phi$ is replaced by unity, the lateral displacement is then given by

$$b\,Cosec 2\alpha\, Sin 2\theta - R\,Sin\theta$$

This in turn for $\theta \to 0$ becomes

$$(2b\,Cosec 2\alpha - R)\theta$$

that is, the lateral displacement is directly proportional to the angle of tilt. The slope of the graph is dominated by the wheelpair taper angle, that is, the smaller the

taper angle, the steeper the graph. This means that for a given wheelpair tilt angle, the smaller the taper angle, the larger would be the lateral displacement of the wheelpair. This information is plotted in Figure 8.1. The left-hand ordinate in this figure shows the lateral displacements as a ratio of the halftrack width while the right-hand ordinate lists the actual displacements. (The taper angle of 2.86^{o} has been included in this figure, since the standard wheel taper on British Railways is 1 in 20.)

It is relevant to comment that the theory shows that the change in the lateral position of the centre of mass is more complex than might at first appear to be the case. Wickens [8] conjectured that:

> the displacement of the centre of mass differs little from that occurring at the wheel.

Inspection of Figure 8.5 shows that the two displacements are not directly related and that such a comparison might be misleading.

8.4.3 Vertical displacement of the centre of mass of the wheelset as it yaws and/or tilts

Using the relationships derived in Section 5.4.4, the displacement in the vertical direction of the centre of mass is:

$$b\text{Tan}\alpha(\text{Sec}\phi-1) + R(1-\text{Cos}\theta) - 2b\text{Cosec}2\alpha\text{Sec}\phi\text{Sin}^2\theta$$

Since $\text{Sec}\phi \to 1$ as $\phi \to 0$ and $\text{Cos}\theta \to 1$ as $\theta \to 0$, the first two terms are negligible for small θ and ϕ, which leaves the third term $-2b\text{Cosec}2\alpha\text{Sec}\phi\text{Sin}^2\theta$, and since this term has a negative sign, this means that as the wheelpair tilts, the centre of mass rises above the position which it occupied in the neutral position when θ was zero; furthermore, for small θ, it is seen that the height of the centre of mass is proportional to the square of the angle of tilt, in addition, the relationship is directly dependent on the cosecant of twice the taper angle of the wheelpair so that

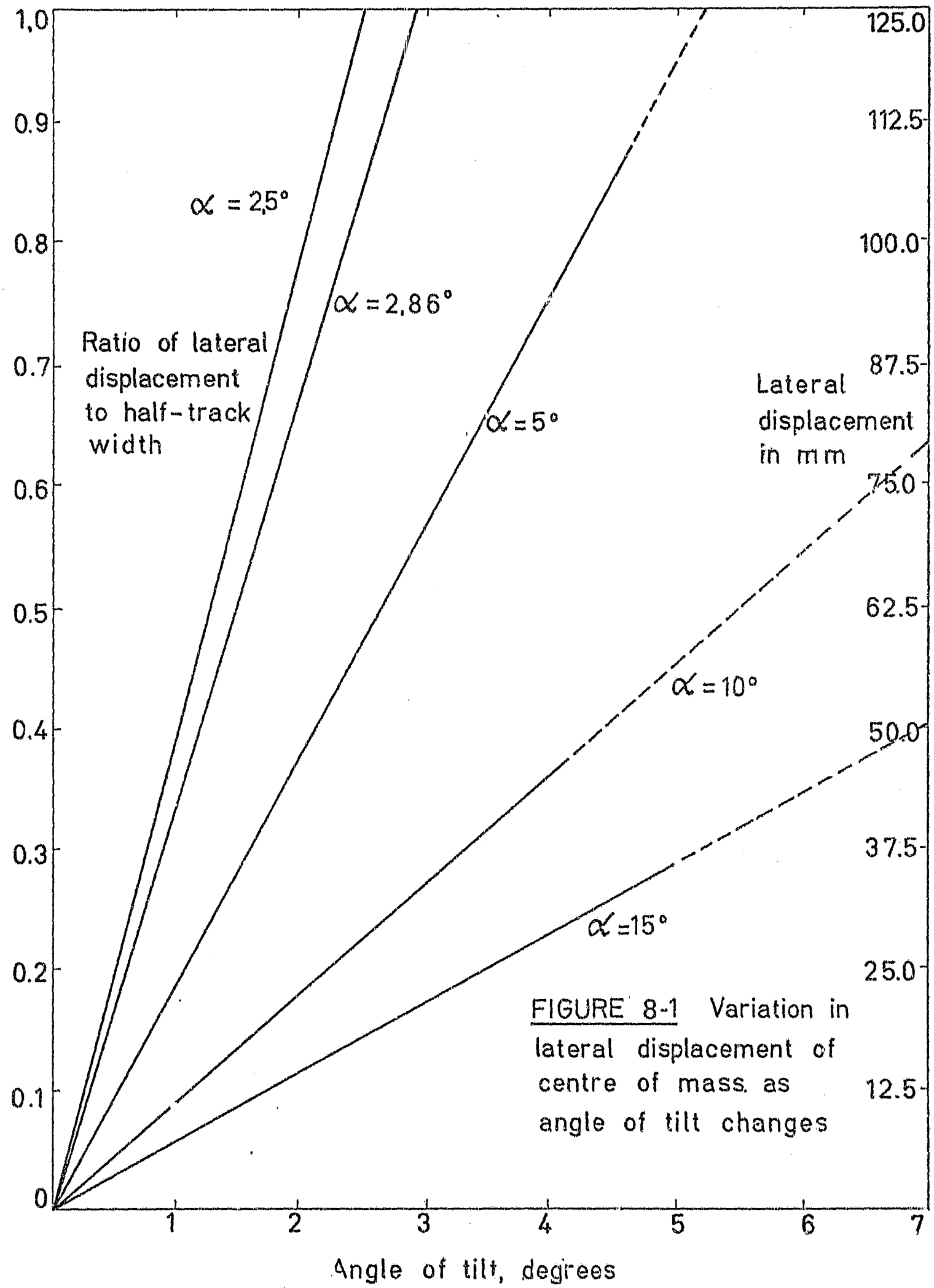

FIGURE 8-1 Variation in lateral displacement of centre of mass as angle of tilt changes

the smaller the taper angle, the larger the vertical displacement of the centre of mass will be. These relationships are shown in Figure 8.2

8.5 CYCLIC CHANGES IN ENERGY IN THE SYSTEM

As the centre of mass of the wheelpair rises above that position which it occupied when the tilt angle was zero, there is a corresponding increase in its gravitational potential energy, a change which is proportional to the square of the angle of tilt of the wheelpair. On the other hand, the potential energy stored in the restraining springs is determined by the square of the angle of yaw of the wheelpair. Since the experimental test runs showed that there was a phase difference of 90°, it can be deduced that, apart from the cyclic changes in kinematic energy, there is a continual interchange in the form of the potential energy in the system. As the angle of tilt of the wheelpair is increased, its gravitational potential energy increases at the expense of the potential energy stored in the restraining springs. Once the gravitational potential energy has reached its maximum (because the angle of tilt is at its maximum value), the potential energy in the restraining springs increases from its minimum value as the angle of yaw in turn changes from zero to its maximum when the cyclic process repeats itself.

This interpretation of the oscillation process is important since it provides an understanding of how the oscillation proceeds. That it is a reasonable hypothesis is seen when the change of height curve for a 30° taper angle is examined. First of all, it is relevent to suggest that in as far as the tilting motion is concerned, the mechanism whereby the oscillation occurs bears some analogy to that of a simple pendulum in a gravitational field. The restoring force in such a pendulum is $-m\ell g\sin\theta$ (where m and ℓ are the mass of the pendulum bob and length respectively), that is, $m\ell g\theta$ as $\theta \to 0$. Unless the restoring force is

greater than the resisting force, motion will not occur. As Figure 8.2 shows, for a cone taper angle of 30°, the change in height of the centre of mass of the dicone is less than 0.2 mm for tilt angles of up to 2°. The restoring force is thus minimal and since there is little possibility that there would be much storage of gravitational energy, one would predict on theoretical grounds that such a dicone would not hunt. This was experimentally confirmed (as indicated in the previous chapter) since the first experiments were conducted with a dicone with a taper angle of 30°. This is then interesting supporting evidence for the validity of the theoretical analysis.

As a further comment, it is important to realize that whereas the restoring force in a simple pendulum is $-m\ddot{\theta}g\theta$ (that is, it is a linear system), the corresponding force in the case of the wheelpair is proportional to θ^2, which is highly non-linear. If an essential element in the mechanism causing hunting has this degree of non-linearity, effecting for example, the amplitude of motion then from this, it can be concluded that it is unlikely that the motion could in any way be represented by a set of linear equations. This would serve to confirm the belief that the linearising procedures used to simplify the differential equations are of dubious validity.

8.6 EXPERIMENTAL CONTACT CONDITION

Whereas the theory assumes that the contact between the wheels and the rails and the two parallel straight rails can be represented as that arising from an idealisation of the latter as occurring along two straight parallel lines, the actual rail surface has a camber of finite radius, so that the positions of the actual points of contact on the test rig would differ from those postulated in the theory. It could be argued that

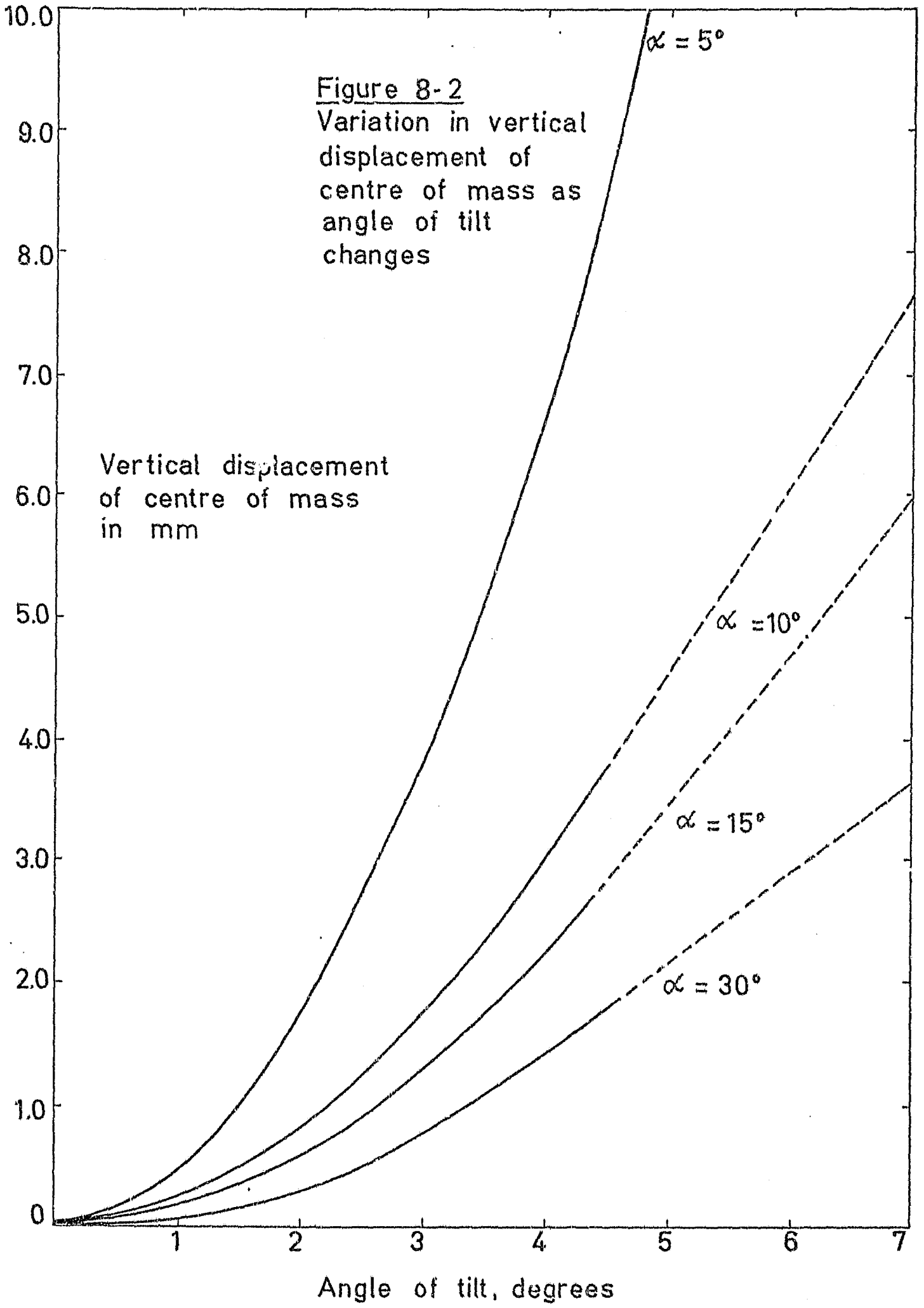

Figure 8-2
Variation in vertical displacement of centre of mass as angle of tilt changes

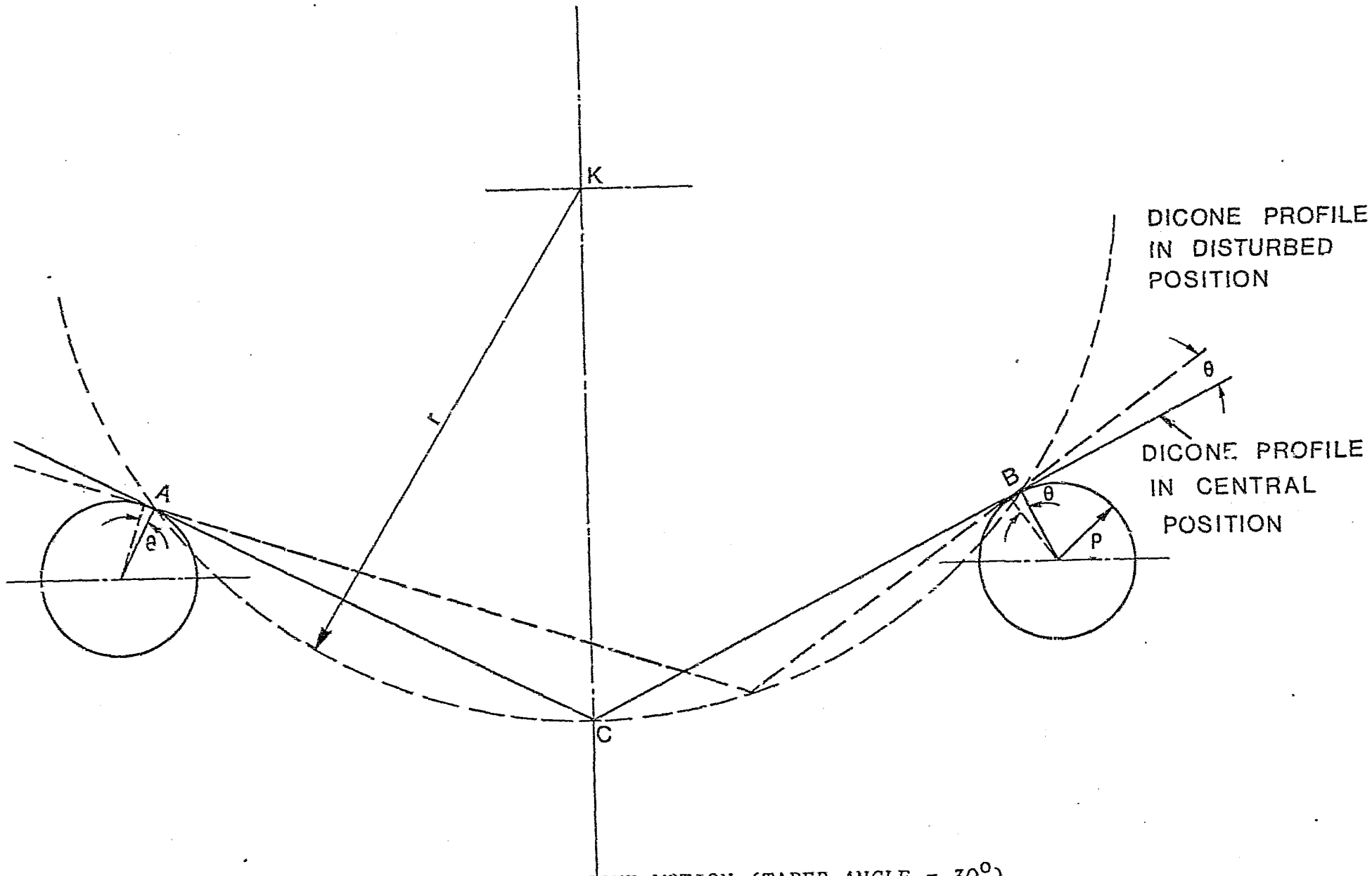

FIGURE 8.3 EFFECT OF RAIL CAMBER ON DICONE MOTION (TAPER ANGLE = 30°)

there is as a consequence a periodic change in the effective rail gauge width during the hunting cycle and that this would be an additional source of difficulty in comparing the theoretical and experimental work.

The validity of such an argument is tested by examining Figure 8.3 where the taper angle has deliberately been taken as 30°. The respective sides of the wheelpair dicone profile are always tangential to the circles which now represent the rails. For an angle of tilt θ and a rail radius ρ, the figure shows that both points of contact would move along the circumferences of the circles representing the rails by the same distance $\rho\theta$; that is, in effect, there is little variation in rail gauge; instead, the rail gauge has a lateral displacement of $\rho\theta\text{Cos}\alpha$. According to the previous section and assuming that the circular arc pattern of the profile motion is unchanged (as the figure indicates even with a steep taper angle, this is not an unreasonable assumption since the displacement of the points of contact is in effect small), the lateral displacement of the centre of the wheelpair would be

$(2b\text{Cosec}2\alpha - R)\theta$

and since in practice

$2b\text{Cosec}2\alpha - R >> \rho^{*}$, (for α small)

so that it is possible to conclude that the supposition that variation in rail gauge, or rather the lateral displacement of the rail gauge, can have the supposed effect is somewhat unjustified. Further, the distance $\rho\theta$ is a small fraction of the actual distance separating the points of contact. In addition, as discussed in a previous section, the yawing and tilting motion (although related to one another by a phase difference) operate in a different manner and since yawing is unlikely to be affected by the rail gauge variation, the overall effect would in any case be minimal.

---

* Using the data given in Appendix 2, $2b\text{Cosec}2\alpha - R$ is 1.35m, which is much larger than any likely value of

8.7 MODEL TESTS AT DERBY

Since the results of the model tests run at Derby by Wickens [8] (already commented on earlier, particularly in Chapter 6) are useful as a basis for comparison with the results achieved here (especially in the light of the characteristic equation derived from the linearized forms of the equations of motion developed in Chapter 5), this section will deal with a summary of his results. Using the equations of motion listed by him for a four-wheeled vehicle, the equations of motion for an isolated wheelpair would reduce to:

$$m\ddot{q}_1 + 2k_2 q_1 = Q_1$$

$$C\ddot{q}_2 + 2b^2 k_1 q_2 = Q_2$$

where

m = mass of wheelset

C = moment of inertia of wheelset in yaw

k_1, k_2 = longitudinal and lateral spring stiffnesses

b = half spacing of suspension mountings for wheelset

ℓ = half distance between contact points in the lateral direction

q_1 = lateral displacement of the wheelset

q_2 = yaw of the wheelset

Q_1, Q_2 = creep forces

f, f' = creep coefficients.

However, Wickens subsequently lists the equations of motion for an isolated wheelset moving along the track at speed V as:

$$m\ddot{q}_1 + 2f'\left(\frac{\dot{q}_1}{V} - q_2\right) + \frac{W}{\ell}(\xi\delta_0 + \varepsilon)q_1 = 0$$

$$C\ddot{q}_2 + 2f\left(\frac{\lambda\ell}{r} + \frac{\ell^2 \dot{q}_1}{V}\right) - W\ell\delta_0 q_2 = 0$$

The second terms represent the creep forces, while the last terms represent 'gravitational stiffness' terms. The spring stiffness terms have vanished and it is possible to conclude that the model isolated wheelset as conceived by Wickens is a wheelpair, with its possibility for yawing motion severely restricted, being pulled along the track by a single central force (which by any standards must be held to be a very unusual type of wheelset). Even stranger is the fact that this is described as 'an elastically restrained wheelset' and that the spring stiffnesses k_1 and k_2 are listed among the parameters of the system. Since the wheelset is so unusual, it is possible that this may have affected the experimental results.

After listing the equations quoted above, Wickens continues:

> For a free motion of the type $q_r = K_r e^{\lambda t}$ the characteristic equation is a quartic and typical solutions of the quartic show that it possesses two large real roots and a pair of complex roots with small modulus. The first large root is associated with a subsidence in lateral translation, the root being approximately
>
> $$\lambda_1 = -2f'/mV$$
>
> The second large root is associated with a subsidence in yaw and in this case
>
> $$\lambda_2 = -2fl^2/CV$$
>
> In practical cases, both subsidences are heavily damped, the time of half amplitude being typically of the order of 0.001 sec. These motions need not, therefore, be considered any further. The pair of complex roots $\mu_3 \pm i\omega_3$ corresponds to a lightly damped oscillation in which the yaw of the wheelset leads the lateral displacement by about a quarter cycle.

In their complete form, the solutions, as suggested by Wickens, are:

$$q_1 = K_{11}e^{-\lambda_1 t} + K_{12}e^{-\lambda_2 t} + K_{13}e^{-\mu_3 t}\mathrm{Sin}(\omega_3 t + \psi_1)$$

$$q_2 = K_{21}e^{-\lambda_1 t} + K_{22}e^{-\lambda_2 t} + K_{23}e^{-\mu_3 t}\mathrm{Sin}(\omega_3 t + \psi_2)$$

where the coefficients K_{ij} are generally determined by the initial conditions. It is understood that the term 'subsidence' refers to a heavily overdamped exponential motion, but it is not al all clear why, or on what grounds, it should be assumed that the coefficients K_{12} and K_{21} are equal to zero. It is the existence of these heavily damped terms which are, in effect, the explanation given by Wickens why the hunting process is a simple harmonic motion.

The description of how the experimental work was done is unhappily brief, but is as follows:

> According to the linear theory, stability can be determined by examining the response to an isolated disturbance. Above the critical speed the amplitude of oscillation eventually grows exponentially with time whereas below the critical speed the amplitude decays exponentially. A sustained oscillation of constant amplitude occurs at the critical speed. The model experiments gave results in accordance with the theory. The roller was run at a given speed and the response of the model to an initial disturbance was examined. This was repeated for different initial deflections to check that the model was behaving in a linear manner. The figure shows the variation of frequency and damping of these responses with speed. The measured critical speed was 22.8 ft/s compared with a value of 24.0 ft/s predicted by theory.

It is assumed that the devices attached to the Dexion angles seen behind the wheelpair in the Derby rig are linear sensing devices for detecting the motion in the yawing and lateral directions. What would have been invaluable as an aid in appreciating the experimental work would have been illustrations showing recordings of these displacements. Nothing approaching exponentially damped motion was observed in the experimental work done here and it is not at all clear why it should have occurred at Derby. There

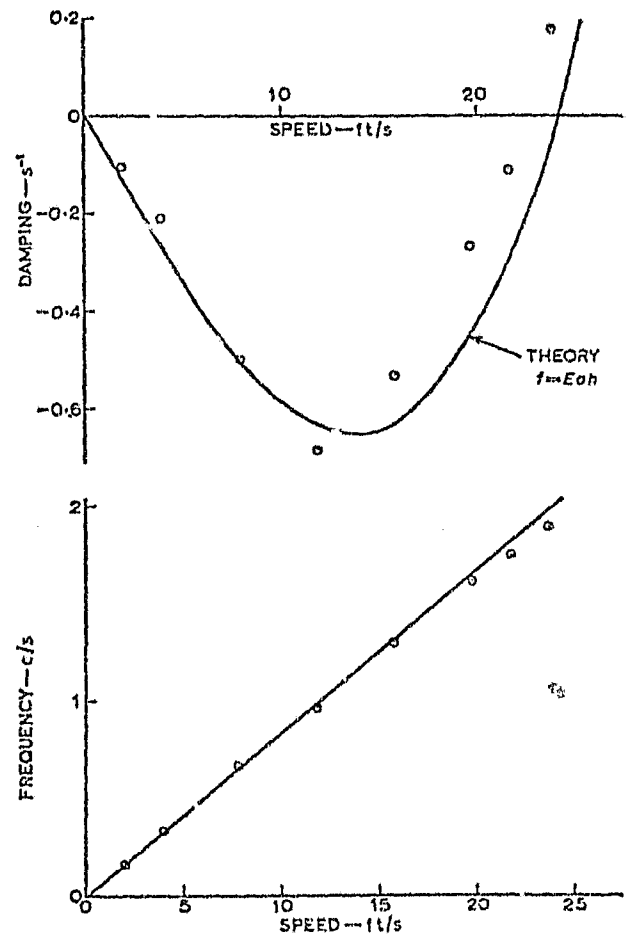

Variation of frequency and damping of transient response of elastically restrained wheelset with speed

ought to be some explanation for the discrepancy in the behaviour of the wheelpairs on the two rigs, but since the necessary Derby facts are lacking, none can be offered.

A final comment is that since the Derby rig was described as an elastically restrained wheelpair, it is surprising that no mention was made of any oscillatory motion in the direction of the longitudinal axis of the aluminium alloy restraining tube. This is the only direction in which elastic restraint is possible, and since with the wheelset this represents a lumped parameter mass-spring linear vibrating system with a disturbing force at the wheel-roller contact surfaces, it would be strange if there were no oscillatory motion in this direction.

8.8 A DISCUSSION OF THE LINEARIZED EQUATIONS OF MOTION

The matrix form of the linearized equation of motion is:

$$\begin{bmatrix} \frac{J_1}{M} + (R-2b\,\mathrm{Cosec}2\alpha)^2 & 0 \\ -\mu b\,\mathrm{Cosec}\alpha\,(R-2b\,\mathrm{Cosec}2\alpha) & \frac{J_1}{M} \end{bmatrix} \begin{bmatrix} \ddot{\theta} \\ \ddot{\phi} \end{bmatrix} + \begin{bmatrix} 0 & \frac{J_3 n}{M} \\ -\frac{J_3 n}{M} & 0 \end{bmatrix} \begin{bmatrix} \dot{\theta} \\ \dot{\phi} \end{bmatrix}$$

$$+ \begin{bmatrix} g(4b\,\mathrm{Cosec}2\alpha - R) & -\mu g\,\mathrm{Sec}\alpha\,(R+b\,\mathrm{Tan}\alpha) \\ 2\mu b g\,\mathrm{Cosec}\alpha & \frac{2KB^2}{M} \end{bmatrix} \begin{bmatrix} \theta \\ \phi \end{bmatrix} = \begin{bmatrix} 0 \\ 0 \end{bmatrix}$$

The leading diagonals in the matrix coefficients of the acceleration column vector and the undifferentiated variable column vector conform to what would be normally expected in such matrices, generally referred to as the inertia and spring matrices respectively. However, in this case, the remaining diagonal terms are Coulomb friction relationships, so perhaps they should be referred to as quasi-inertia and quasi-spring matrix coefficients. The intermediate matrix coefficient, that is, the matrix attached to the velocity column vector, is the classic gyroscopic matrix; thus Meirovitch [31] shows that if gyroscopic forces occur in a dynamic system, the matrix coefficient of the generalized velocities is always skew-symmetric. The reason for this is that the gyroscopic forces do no work in the system. Meirovitch adds:

> As it turns out gyroscopic stabilization is possible only if the original system is conservative. Indeed in the presence of dissipative forces, this type of stabilization is lost.

It is interesting to compare the matrices derived above (referred to in the subsequent discussion as the derived coefficients) with the corresponding coefficients for the equations of motion which were developed by Wickens and

Brann and which were quoted in chapter 4. In making the comparison, it has to be remembered that the generalised coordinate q_1 is the lateral displacement which corresponds to the angle of tilt θ used in this work, while the other generalised coordinate q_2 is the yaw here designated as ϕ.

There is a distinct similarity in all the inertia matrices with regard to the leading diagonal - thus the moment of inertia C corresponds to the term $\frac{J_1}{m}$. Since this work uses an angular displacement instead of a linear displacement for the other coordinate, the derived element is a moment of inertia removed from the principal axis in the place of the mass. The derived reverse diagonal shows a friction dependent element in the place of the zeroes in the Wickens and Brann matrices. The friction dependent element is related to the angle of tilt, which is not altogether surprising since the normal forces vary with the angle of tilt (and only marginally with the angle of yaw) and these forces would then have a bearing on the acceleration experienced by the wheelpair. It is, of course, possible to assert (based solely on an intuitive analysis of the physics of the motion) that similar inertial effects would accompany the yawing motion and that for that reason, a corresponding coupling term in respect of yaw should be found in the inertia matrix. Unfortunately, intuition is not always an adequate guide nor is it axiomatic that one's grasp of the physics of the motion is sufficient to make such predictions possible. In this case, the supposition that such a term should be present would not appear to be a logical deduction.

Turning to the spring matrices, it would seem that Brann's matrix coefficient is incomplete. The derived matrix and that proposed by Wickens are similar in that the stiffness (both spring and gravitational) elements in the leading diagonal resemble each other. There are creep dependent elements in the reverse diagonal in one case and dry friction elements in the other. The major discrepancy lies in the velocity vector matrix coefficient where both Brann and Wickens have symmetric

matrices, whereas the derived matrix is skew symmetric.

What is surprising in such a discussion is that there is sufficient resemblance between the various matrix coefficients to make it likely that the subsequent characteristic equations would appear to be similar and that in the case where creep coefficients were used, a suitable adjustment of the data would produce characteristic roots which would agree with the frequencies met in practice. Indeed, the equations themselves have doubtless been efficacious in providing a realistic and practical basis for analysis leading to design. However, this is not the point at issue in this work, where the aim has been towards an improved understanding of the mechanism responsible for railway hunting. It is remarkable, for example, that gyroscopic forces should have been ignored elsewhere.

8.9 THE SOLUTION OF SIMULTANEOUS NON-LINEAR DIFFERENTIAL EQUATIONS

Since all the evidence suggests that the hunting cycle is non-linear, it is apparent that adequate solutions are not forthcoming from the linearised forms of the equations set out in section 5.9.4 and 5.11.2. By stripping these equations of second and higher order terms, manageable equations had been obtained, but the equations in their original form are lengthy and complicated; thus, the equations of angular motion occupy no less than two pages of the text. It might be possible by a judicious elimination of some of the terms to reduce the equations somewhat, but such an attempt could only be undertaken by someone whose expertise lay in the solution of such complex non-linear differential equations.

A further complication is that the weakest link in the argument put forth is that, following Coulomb's law, there is simple proportionality between the tractive frictional force and the normal force. This is, however, a problem which has up to the present frustrated all researchers and if all the possible variables are to be included, it is likely to prove insoluble.

Any attempt to improve on the Coulomb law would merely add to the existing difficulties.

The solution of even relatively weakly non-linear differential equations is fraught with problems, although the equivalent linearisation methods proposed by Bogoliubov and Mitropolsky [47 , pp 115 - 143] have in certain instances proved successful. Nevertheless, it is significant that the warning should be given on page 144:

> The asymptotic methods described so far are limited in the application to the requirement that the relevant equations are to contain a small parameter.

It is pointed out by Butenin [48] that;

> The study of the bahaviour of a self-excited system with several degrees of freedom under the influence of an external sinusoidal force is a very complicated problem.

He then proceeds to a study of a non-linear system which approximates closely to a linear, conservative system and then imposes two further limitations so as to make analysis possible. Even with these simplifications the resulting conclusions are complex and difficult to interpret. The problem posed by Lord Kelvin [49] ('On the Dependence of the Motion of a Clock on its Means of Suspension') is used to illustrate the methods involved. Despite the simplification and despite the choice of a problem amenable to the methods available to him, Butenin has reservations about the outcome, thus:

> In conclusion, we note that experimental studies of this phenomenon qualitatively varify the theory. It would be impossible to demand a quantitative agreement with experiment because of the assumptions on which the theory is based and, most of all, because the forces of friction and the operation of the suspension mechanism differ greatly from the way in which a pocket watch works.

These comments confirm what has been stated in the opening paragraph to this section, that is, given enough skill, it is likely that the differential equations could be adequately interpreted. Nevertheless, much supporting evidence has been obtained to justify the belief that the underlying theory is solidly established and that the equations are representative of the dynamic behaviour of the wheelpair.

CHAPTER 9

AN OVERALL REVIEW OF THE HUNTING PROBLEM

The side-to-side movement which occurs under certain conditions (and which is often referred to as railway hunting) of a railway wheelpair as it travels along a straight pair of rails has interested many workers over a long period of time. It is a problem of great complexity so that despite efforts which have been made to fully comprehend the phenomenon, no final solution has yet been produced. In this work, an attempt has been made to approach the problem in a manner which is different to those which have been followed elsewhere. The model investigated has been reduced - in so far as this is possible - to its basic elements, thus, it has been limited to examining the behaviour of an unflanged wheelpair with uniformly tapering running surfaces caused to travel along a straight pair of rails with spring restraint placed on its shaft bearings.

As is the case in all dynamic problems, the motion of the wheelpair is determined by the nature of the forces applied to it. The character of these forces is open to different interpretations and it is at this point that this work is at its most contentious. Whereas it has been believed since Carter first put forward his hypothesis of creep - which then became a paradigm or traditional practice - that this was a form of progress intermediate between rolling and sliding, it is claimed here that the duration of this occurrence is extremely brief. Either the wheelpair adheres to the rail at the points of contact

and has pure rolling motion in the neutral position mid-way between the rails, or, the adhesion is lost; the rate at which the wheelpair rotates is diminished and it then proceeds to slide across the rails with a transverse oscillatory type of motion. It is the supposition of this work that it is the manner in which adhesion is lost which is the phenomenon described in the literature as creep. The time taken for adhesion to be lost is extremely brief and it is not the case, as is generally put forward in the literature, that it is of significance in determining the nature of the oscillatory movement.

Since it is presumed that the wheelpair always maintains contact with the rails, it is possible, by using a geometrical analysis which has reference to a particular set of coordinate axes, to establish the position of the centre of mass of the wheelpair at any time as a function which has the angles of yaw and tilt as its variables. The coordinates of the two points of contact between the wheels and the rails in the given space can be found. These coordinates are used as position vectors to determine the wheelpair surface velocities at the points of contact as functions of the angles of yaw and tilt. These equations show that unless the wheelpair is in the neutral position with zero angles of tilt and yaw, it has to slide over the rails.

As a consequence of this finding, it has been assumed that the forces at the points of contact are dry frictional tangential forces acting in the direction of the rails and that they are proportional to the normal forces at these points. Two of the three equations of linear motion - one in each coordinate axis direction - are used to find the normal forces and the remaining equation then provides the equation governing linear motion of the wheelpair in the direction of the rails. Sufficient information has in this way been gained so that the equations governing the angular motion of the wheelpair can be found. If the assumption is made that these somewhat involved equations can be linearised, then it can be shown that there is

no cross-coupling between the longitudinal linear motion and the angular movements.

The validity of the theoretical conclusions rested on supporting evidence obtained from experimental test runs. For practical reasons, experiments had to be conducted in such a manner that instead of the wheelpair travelling along a track, it was held under elastic constraints and the 'track' made to move so as to obtain the required relative motion between the wheelpair and itself. In all experiments conducted elsewhere on so-called roller rigs, the relative track movement is produced by allowing the wheelpair to rotate by placing it on top of a pair of driven rollers. Since the nature of the motion over the range of contact between the wheelpair and the rollers is held to be dissimilar to that which would occur if the wheelpair were made to travel along a straight track, an alternative form of testing method was sought. After some trail-and-error approaches it was found possible to construct a rig in which the motion in the range of possible contacts between the wheelpair and the rail simulating surfaces was of the linear form encountered in reality. This was achieved by using a travelling metal belt supported on an air cushion. An aspect of the motion, which had been overlooked in the original design, was the need for adequate lateral guidance of the rail simulating surface to oppose the inertial forces in the wheelpair as it oscillated laterally, but once this problem had been recognized, appropriate means were found to provide adequate lateral support for the 'rails'.

After initial test runs had confirmed the theoretically determined conclusion that no coupling existed between the linear motion of the wheelpair in the direction of the track and its angular motion, a yoke was installed on the rig which allowed the wheelpair to yaw and to tilt freely but which effectively prevented the unwanted lateral movement. A variety of methods were used to confirm that the motion was simple harmonic with a 90° phase shift between the yawing and tilting movements.

Provided that the rail speed exceeded a certain critical figure, the wheelpair would start to oscillate spontaneously without outside interference. Within the range of speeds at which the rig could be operated, the amplitudes of the oscillatory motion increased somewhat with increase in rail-speed up to a certain maximum. The behaviour of the wheel-pair when it was disturbed from the pure rolling, or neutral, position in the absence of yaw or tilt was investigated; that is, at rail speeds below the critical speed. It was found that the wheelpair after a number of oscillatory cycles (the actual number increasing as the rail speed increased) the wheelpair would revert abruptly to pure rolling motion; that is, the adhesion which had formerly been lost was recovered. A possible explanation as to why this was more likely to occur at lower speeds was that it was easier at these speeds for a match to be obtained between the belt speed and the wheelpair surface speed. At higher speeds, this matching became less easy until at the critical speed, this facility was lost.

It is suspected that the non-linearity of the equations of motion is such that sophisticated methods of solution are required to obtain solutions to the differential equations of motion. This view is supported by the fact that the gravitational potential energy is a significant element in the mechanism of the oscillatory motion - and this is, in turn, dependent on the s f the angle of tilt. The oscillatory motion would pear to be a form of limit cycle. Although the linea equations of motion show several interesting features - thus the matrix coefficient of the linear velocity vector is of the classic gyroscopic matrix form - it is believed that the data derived from the characteristic equation, which is based on the linearised form, should not have too much emphasis placed on it. The value of the experimental frequency was about 16% higher than the higher of the two theoretically predicted natural frequency. This suggests that it is likely that the

frequency of the limit cycle would approximate to the experimental value. To place any reliance on the possibility that the real parts of the roots derived from the frequency equation would give any guidance as to the stability, or otherwise, of the system would not appear to be justified. The gravitational energy exchange element in the oscillatory process probably determines the maximum amplitude of the limit cycle. It is of interest that the experimental frequency of oscillations did not vary whereas the linearised forms of the equations suggest that this would be the case. This again confirms the likelihood that such equations provide an incomplete guide to the response of the dynamic system.

The characteristic roots of the linearized equations have been listed in Appendix A3 for various spin speeds and coefficients of friction. A comparison of the first harmonic frequencies and the experimental frequency is given in Appendix A4 while Appendix A8 shows how the validity of the roots given in Appendix A3 has been verified.

REFERENCES

1. HEADING, J. *Matrix Theory for Physicists*, London, Longmans, 1958

2. CHIRGWIN, B and PLUMPTON C. *A Course of Mathematics for Engineers and Scientists*, Vol 6, London, Pergamon, 1966

3. PARS, L A. *A Treatise on Analytical Dynamics*, London, Heineman, 1965

4. D'ABRO, A. *The Rise of the new Physics*, New York, Dover, 1951, pp 14,15

5. PLANCK, M. *Where is Science going?* London, Allen and Udwin, 1933, p 82, (English translation)

6. HAMMOND ELLIS, C. *The Lore of the Train*, London, Allen and Udwin, 1971

7. LOMONOSOFF, G V. *Introduction to Railway Mechanics*, London, O.U.P. 1933

8. WICKENS, A H. The Dynamics of Railway Vehicles on Straight Track: Fundamental Considerations of Lateral Stability, *Proc. Inst. Mech. Engrs.*, 180 (1965/6) S.F., pp 29-44, 67-72

9. MARRIS, W A and STONEKING, C E. *Advanced Dynamics*, New York, McGraw Hill, 1967

10 MacMillan, W. D. 'Dynamics of Rigid Bodies' New York, Dover, 1960

11 Huddleston, J. V. 'Introduction to Engineering Mechanics' Reading, Addison - Wesley, 1961

12 Klingel, "Über den Lauf der Esienbahnwagen aug gerarder Bahn' Organ, Fortshr, Eisenbah Wis, 38, 113 - 123, 1883

13 Rocard, Y. 'General Dynamics of Vibrations', London, Lockwood, 1960

14 Inglis, Sir C. 'Applied Mechanics for Engineers', Cambridge, C.U.P, 1951, pp 193 - 5

15 Schutzbach, H., 'Probleme der Bestimmung der Beruhrungs Verhaltnissen von Rad und Schienen'. Erforschung der Grenzen des Rad/Schiene Systems', Munich, 1974

16 Levi, R. 'Etude Relative au Contact des Roues sur le Rail', Revue General des Chemins de Fer, February 1935 pp 81 - 109

17 Klein, F and Sommerfeld, A. "Über der Theories des Kreisels', New York, Johnson Reprint, 1965

18 Kuhn, T.S. 'The Structure of Scientific Revolutions' 2nd Edition enlarged, Chicago, 1970

19 Kuhn, T.S. 'The Essential Tension', Chicago, University of Chicago Press, 1977

20 Popper, K. 'The Logic of Scientific Discovery', London, Hutchinson, 1972

21 Medawar, P. 'The Philosophy of Karl Popper', Proc. of the Royal Inst. of Gt. Britain, Vol. 50, 1978

22 Carter, F.W. 'Railway Electric Traction', London, Arnold, 1922, pp 57 - 70

23 Swift, H.W. 'Power Transmission by Belts', Proc. Inst. of Mech. Eng., 1928, Vol. II

24 Reuleaux, F. 'The Kinematics of Machines', Trans. and Edt. by Kennedy, A.B., New York, Dover, 1963

25 Green, W.G. 'Theory of Machines', 2nd Edition, London, Blackie & Son, 1962

26 Johnson, K.L. 'The Effect of a Tangential Contact Force upon the Rolling Motion of an Elastic Sphere on a Plane', J. Applied Mech., Sept. 1958, pp 339 - 346

27 Vermeulen, P.J., and Johnson, K.L, 'Contact of Non-Sperical Elastic Bodies Transmitting Tangential Forces', Trans. A.S.M.E., June 1964, pp 338 - 340

28 Kalker, J.J. 'On the Rolling of Two Elastic Bodies in the presence of Dry Friction', Doctoral Thesis, Delft Technological University, 1967

29 Wickens, A.H. 'General Aspects of the Lateral Dynamics of Railway Vehicles', Journ. of Eng. for Ind., 1969, pp 869 - 878

30 Wickens, A.H. 'The Dynamic Stability of Railway Wheelsets and Bogies having Profiled Wheels', Int. J. Solids and Struct., 1965, Vol. 1, pp 319 - 41

31 Brann, R.P. 'Some Aspects of the Hunting of a Railway Axle', J. Sound and Vibr., 1964, 4(1), pp 18 - 32

32 Benington, C.K. 'The Railway Wheelset and Suspension unit viewed as a closed loop guidance control system': A method for performance improvement, Journ. Mech. Eng. Sc., Vol. 10, No. 2, 1968

33 Royer, M. 'Recherches sur les Proprietes dynamiques d'un Dicone se Deplacement en Alignement droit,' Bull Assn. Int. Cong. Chemin de Fer, pp 801 - 16

34 Heinze, S. and Albrecht, H. 'Probleme der Bestimmung der Kraftschlussbeuverte anzuwendende Haftwerttheorie und Bestatigung der Haftwerttheorie durch Versuche', Erforschung der Grenzen des Rad/Schiene Systems, Munich, 1974

35 Savage, M. and Loewenthal, S.H. 'Kinematic Stability of Roller Pairs in Free Rolling Contact', Nasa. Tech. Note, TN 8146

36 Davies, R.D. 'Some Experimerts on the Lateral Oscillation of Railway Vehicles', J. Inst. Civ. Engrs. 11, 1939, pp 224 - 257

37 Althammer, K. 'German Ministry Roller Test Plant at Munich', Railway Engineer, Vol. 2, No. 5, Sept/Oct 1977, pp 15 - 24

38 Salter, J.P. 'Steady State Vibration', London, Kenneth Mason, 1969

39 Anon. 'Feasibility Study for a Wheel-Rail Dynamics Research Facility', Bull. of the International Railways Congress Assn., July/Aug 1969, p 464

40 Matsudaira, T., Matsui, N, Arai, S and Yokose, K. 'Problems on Hunting of Railway Vehicles on Test Stand', Journal of Eng. for Indus., August 1969, pp 879 - 890

41 Grassam, N.S. and Powell, J.W., 'Gas Lubricated Bearings', London, Butterworth, 1964

42 Kharlamov, P.V. 'New Methods in the Dynamics of Systems of Rigid Bodies', IUTAM Symposium, Munich, 1977

43 Bishop, R.E.D., Gladwell, G.M.L. and Michaelson 'The Matrix Analysis of Vibration', Cambridge, C.U.P 1965, page 73

44 Francis, J. 'A History of the English Railway - Its Social Relations and Revalations', London, Longman Brown, Green and Longmans, 1851

45 Collins, A.H. and Pritchard, C. 'Recent Research in Adhesion', Railway Eng. Journ., Sept 1972, pp 19 - 23

Meirovich, L. 'Methods of Analytical Dynamics', New York, McGraw Hill, 1970

47 Bogoliubov, N. N. and Mitropolsky, P. 'Asymptotic Methods in the Theory of Non-Linear Oscillations', Delhi, Hindustan Pub. 1961

48 Butenin, N.V. 'Elements of the Theory of Non-Linear Oscillations', New York, Blaisdell, 1965

49 Thomson, W. (Kelvin), 'Popular Lectures and Addresses' London, Vol. 2, 1894

APPENDIX 1

DATA FOR EXPERIMENTAL WHEELPAIR

α = 5°

b = 0.124 6 m

B = 0.286 5 m

M = 10.45 kg

k = 117 N/m

r' = Mean running radius = 0.085 75 m

J_1 = 0.215 kg m^2

J_3 = 0.145 5 kg m^2

APPENDIX A2

The characteristic equation in terms of the rig data is:

$$\frac{J_1 J_1^*}{M^2}s^4 + \frac{J_3 n}{M}\mu b R^* \text{Cosec}\alpha s^3 + \{\frac{J_1}{M}(2b\text{Cosec}2\alpha + R^*) + \frac{2J_1^* kB^2}{M^2} +$$

$$(\frac{J_3 n}{M})^2 - 2\mu^2 b R^* \text{Cosec}2\alpha(R + b\text{Tan}\alpha)\}s^2 - \frac{J_3}{M}\mu n g\{R\text{Sec}\alpha + b\text{Cosec}\alpha(1 +$$

$$\text{Sec}^2\alpha)\}s + \frac{2kB^2}{M}g(2b\text{Cosec}2\alpha + R^*) + 4\mu^2 g^2 b\text{Cosec}2\alpha(R + b\text{Tan}\alpha) = 0$$

Using the following test rig values,

$\alpha = 5^o$	$k = 117$ N/m
$M = 10.45$ kg	$b = 0.124\ 6$ m
$J = 0.215$ kg m^2	$B = 0.286\ 5$ m
$J = 0.145\ 5$ kg m^2	$R = 0.086\ 68$ m

we have

$R^* = 2b\text{Cosec}2\alpha - R = 1.435\ 056 - 0.086\ 68 = 1.348\ 406$

$$R^* + 2b\text{Cosec}2\alpha = 1.435\ 056 + 1.348\ 406 = 2.783\ 491$$

$$J_1^* = J_1 + MR_1^{*2} = 0.215 + 10.45 \times 1.348\ 406^2 = 19.215\ 166$$

$$R + b\text{Tan}\,\alpha = 0.866\ 68 + 0.124\ 6\ \text{Tan}\ 5^o = 0.097\ 811$$

$$\frac{J_1 J_1^*}{M^2} = \frac{0.215 \times 19.21\ 152}{10.15} = 0.037\ 831$$

$$\frac{J_3}{M}\mu nbR^*\text{Cosec}\alpha = \frac{0.145\ 5}{10.45} \times 0.124\ 6 \times 1.348\ 406\ \text{Cosec}\ 5^o \times \mu n$$

$$= 0.028\ 404\ \mu n$$

$$\frac{J_1}{M}g(2b\text{Cosec}2\alpha + R^*) = \frac{0.215}{10.45} \times 9.81 \times 2.783\ 491$$

$$= 0.561\ 799$$

$$2kJ_1^* \frac{B^2}{M^2} = \left(\frac{0.286\ 5}{10.45}\right)^2 \times 2 \times 117 \times 19.215\ 166$$

$$= 3.379\ 688$$

$$\left(\frac{J_3 n}{M}\right)^2 = \left(\frac{0.145\ 5}{10.45}\right)^2 n^2 = 0.000\ 193\ 86\ n^2$$

$$2\mu^2 bgR^*\text{Cosec}2\alpha(\Gamma + b\tan\alpha) = 2 \times 0.124\ 6 \times 9.81 \times 1.348\ 406 \times 0.097\ 811\ \text{Cosec}\ 10^o\ \mu^2$$

$$= 1.852\ 393\ \mu^2$$

$$\frac{J_3}{M}n\mu g\{R\text{Sec}\alpha + b\text{Cosec}\alpha(1+\text{Sec}^2\alpha)\} = \frac{1.145\ 5}{10.45} \times 9.81\{0.086\ 68\ \text{Sec}\ 5^o + 0.124\ 6\ \text{Cosec}\ 5^o(1+\text{Sec}^2 5^o)\}\mu n$$

$$= 0.403\ 924$$

$$\frac{2kB^2}{M}g(2b\text{Cosec}2\alpha + R^*) = \frac{234}{10.45} \times 0.286\ 5^2 \times 9.81 \times 2.784\ 9$$

$$= 50.188\ 901$$

$$4\mu^2 g^2 b\text{Cosec}2\alpha(R + b\text{Tan}\alpha) = 26.953\ 271\ \mu^2$$

The 1st and 3rd order terms involve the product μn. The ratio of these terms is:

$$\frac{bR^{*}Cosec\alpha}{g\{RSec\alpha+bCosec\alpha(1+Sec^{2}\alpha)\}} = \frac{0.124\ 6}{9.81} \times \frac{15.471\ 122}{2.957\ 203}$$

$$= 0.066\ 450$$

Hence the characteristic equations in terms of the system parameters (but leaving μ and n unspecified) is:

$$0.037\ 831s^{4} + 0.028\ 404\ \mu ns^{3} + (0.561\ 799 + 3.379\ 688$$

$$+ 0.000\ 193\ 86\ n^{2} - 1.852\ 393\ \mu^{2})s^{2} - 0.403\ 924\ \mu ns$$

$$+ 50.188\ 901 + 26.953\ 271\ \mu^{2} = 0$$

First and third order terms for three values of μ and three values of n:

Order of term	n	μ = 0.05	μ = 0.10	μ = 0.40
3rd	28.46	0.038 194	0.076 378	0.305 551
	50	0.067 101	0.134 202	0.536 808
	100	0.134 202	0.268 404	1.073 617
1st	28.46	0.574 780	1.149 560	4.598 241
	50	1.009 804	2.019 607	8.078 428
	100	2.019 607	4.039 214	16.156 857

Value of 2nd order term for various μ and n, (as given by $3.941\ 486 + 0.000\ 193\ 86\ n^{2} - 1.852\ 393\ \mu^{2}$):

n	μ $-1.852\ 393\,\mu^2$ $0.000\ 193\ 86\ n^2$	0.05 -0.000 046	0.10 -0.001 852	0.40 -0.029 634
28.6	0.158 570	4.100 011	4.098 205	4.070 419
50.0	0.484 650	4.426 091	4.424 285	4.396 499
100.0	1.933 839	5.875 301	5.856 802	5.845 688

Value of constant term for various values of μ

μ	$50.188\ 901 + 26.953\ 271\ \mu^2$
0.05	50.256 284
0.10	50.458 433
0.40	54.501 424

The characteristic equations for various values of μ and n are then as follows:

n = 28.46, μ = 0.05

$$0.037\ 831s^4 + 0.038\ 194s^3 + 4.100\ 011s^2 - 0.574\ 780s + 50.256\ 284 = 0$$

n = 50.0, μ = 0.05

$$0.037\ 831s^4 + 0.067\ 101s^3 + 4.426\ 091s^2 - 1.009\ 804s + 50.256\ 284 = 0$$

n = 100.0, μ = 0.05

$$0.037\ 831s^4 + 0.134\ 202s^3 + 5.875\ 301s^2 - 2.019\ 607s + 50.256\ 284 = 0$$

$\underline{n = 28.46,\ \mu = 0.10}$

$$0.037\ 831s^4 + 0.076\ 378s^3 + 4.098\ 205s^2 - 1.149\ 560s + 50.458\ 433 = 0$$

$\underline{n = 50.0,\ \mu = 0.10}$

$$0.037\ 831s^4 + 0.134\ 202s^3 + 4.424\ 285s^2 - 2.019\ 607s + 50.458\ 433 = 0$$

$\underline{n = 100.0,\ \mu = 0.10}$

$$0.037\ 831s^4 + 0.268\ 404s^3 + 5.856\ 802s^2 - 4.039\ 214s + 50.458\ 433 = 0$$

$\underline{n = 28,46\ \ \mu = 0.40}$

$$0.037\ 831s^4 + 0.305\ 551s^3 + 4.070\ 419s^2 - 4.598\ 241s + 54.501\ 424 = 0$$

$\underline{n = 50.0,\ \mu = 0.40}$

$$0.037\ 831s^4 + 0.536\ 808s^3 + 4.396\ 499s^2 - 8.078\ 428s + 54.501\ 424 = 0$$

$\underline{n = 100.0,\ \mu = 0.40}$

$$0.037\ 831s^4 + 1.073\ 617s^3 + 5.845\ 688s^2 - 16.156\ 857s + 54.501\ 424 = 0$$

The solutions of the roots of these nine quartics are embodied in Table 7.1.

APPENDIX A.4

THEORETICAL FIRST HARMONIC AND EXPERIMENTAL FREQUENCIES AT VARIOUS SPIN SPEEDS AND RAIL SPEEDS (WHEEL DIAMETER = 0.8 m)

μ	n(rad/s) n(r/min) Rail speed (km/h)	28.46 271.8 40.99	50.0 477.5 72.0	100.0 954.9 144.0
0.05	Frequency (rad/s)	9.72	10.21	11.99
0.10	Frequency (rad/s)	9.72	10.20	11.78
0.40	Frequency (rad/s)	9.53	8.88	---
Final Experimental Frequency (rad/s)		11.3	11.3	---

APPENDIX A.3

CALCULATED ROOTS OF CHARACTERISTIC EQUATIONS FOR VARIOUS VALUES OF SPIN SPEED AND COEFFICIENTS OF FRICTION

	0.05		0.10		0.40	
n = 5 rad/S	0.0377 ± j3.8558	-0.1316 ± j9.4513	0.0763 ± j3.8726	-0.2640 ± j9.4252	0.3964 ± j4.2150	-1.1472 ± j8.8915
n = 10 rad/S	0.0746 ± j3.8439	-0.2623 ± j9.4765	0.1503 ± j3.8543	-0.5257 ± j9.4536	0.6870 ± j4.0310	-2.1887 ± j9.0204
n = 20 rad/S	0.1428 ± j3.7980	-0.5182 ± j9.5758	0.2834 ± j3.7867	-1.0342 ± j9.5619	1.0232 ± j3.6442	-4.0264 ± j9.1858
n =28.46rad/S	0.1813 ± j3.7376	-0.6861 ± j9.7160	0.3530 ± j3.7025	-1.3625 ± j9.7244	1.0581 ± j3.3483	-5.0964 ± j9.5320
n = 50 rad/S	0.2633 ± j3.5365	-1.1501 ±j10.2132	0.4981 ± j3.4581	-2.2718 ±j10.2033	1.2622 ± j2.8449	-8.3571 ± j8.8815
n = 100 rad/S	0.3037 ± j2.9714	-2.0774 ±j12.0216	0.5698 ± j2.8715	-4.1172 ±j11.7761	1.3397 ± j2.1042	-12.4242/-18.6346

Note: The validity of the roots listed have been tested as shown in Appendix A8.

APPENDIX 5

The problem of the determination of the force transmission coefficients; relative locked zone theory and the experimental evaluation of the locked zone theory.

by Siegfried Heinze and Hans Albrecht

(Since this appendix is concerned only with the basic concepts, the mathematical development with the accompanying figures has been omitted.)

1. INTRODUCTION

In the past - and even in more recent times - the oscillatory motion (the sinusoidal path) of the wheelpair travelling along a straight pair of rails has been approached as if it were a kinematic problem, that is, in terms of the geometric displacements of the wheelpair as a function of the outline or profile of the wheelpair tyre. The relationship was mathematically discussed for the single wheelpair by Klingel and by Heumann for the multi-wheelpaired arrangement. These treatments envisaged nevertheless, rolling without slip, an assumption not substantiated by closer investigation of the progression of the wheel, since in the course of the motion, the wheelpair and parts of the attached spring supported masses swing in a direction transverse to the rails. The horizontal forces produced by the attached spring-connected masses cause the wheelpair to creep across the rails.

In addition to the transverse creep, there is for the driven wheelpair, a creep in the rail direction. The

resultant slip vector can therefore take up any position within the contact area. It is therefore not possible to determine the wheelpair motion solely by means of kinematic considerations. A dynamic approach must therefore be added to complement the kinematic treatment.

If the wheelpair is thought of as part of a coupled multi-mass system, the mathematical consequences of the system motion as caused by the applied forces and moments can be investigated. For the equations of motion, there must, in addition to the geometrical relationships, be allowances for the frictional forces. This complicating addition then leads to second order differential equations where, in addition to the numerical evaluation of the spring and damping constants as well as the geometrical relations, it is necessary to determine what mathematical relationships regulates the forces transmitted across the contact surfaces.

Since simultaneous transverse and longitudinal slip occurs not only in driven wheelpairs but also in every curve as well as during oscillatory motion, a precise knowledge of the force transmitted as a function of the direction of slip is required.

2. THE LATEST RESULTS OF THE CREEP FORCE INVESTIGATIONS MADE BY KALKER AND FREDERICK

Ever since creep forces have been investigated, many prominent researchers have occupied themselves with this problem area wherein nevertheless the main thrust has been to investigate the magnitude of the limiting slip force. In a historical review of the development of slip force investigation, one would quote names like Andrews, Cabble, Koffman and Krettek.

A comprehensive investigation into the creep force relationships has been professionally concluded by the work of Kalker and Frederick.

2.1 THEORETICAL FUNDAMENTALS

2.1.1 Normal stress distribution

Through his investigations, H Hertz laid the first theoretical basis for creep force research. The objects of the investigation were two elastic bodies pressed together by a normal force N so that between them a contact surface as shown in Figure 1* would be formed. It was assumed that no friction existed between the surfaces and the boundary conditions for the bodies could be approximated by elliptic paraboloids. The contact surface is as a consequence an ellipse while the form of the stress distribution pattern is elliptical.

2.1.2 The relationship between surface stresses and displacements for the three dimensional problem

In his book 'A treatise on the mathematical theory of elasticity', Love succeeded in finding a relationship between the surface stresses and the three dimensional displacements of two bodies of arbitrary curvature rolling over one another.

Two semi-infinite elastic bodies are considered which move over an elliptic contact surface.

(Here follows a mathematical analysis.)

---

* Not given in this translation

2.2 LOCKED ZONE OR ADHERENCE THEORY (KALKER)

The numerical procedure set out by Kalker in his thesis makes it possible to establish the forces entailed for any given spin, slip and arbitrary creep direction. Like Love, he assumes (or approximates) that the two bodies moving relative to one another are elastic and semi-infinite. Using the assumption that the tangential force does not affect the normal stress distribution (which is supported by the work done by de Pater for bodies having the same elastic properties), it is possible, using the theory of Hertz to relate the semi-axis of the elliptic contact surface to the normal stress. As was assumed by Carter, Kalker uses a constant creep coefficient and as a consequence of the analytical procedure, the contact surface is then separated into a locked region and a slip region (as shown in Figure 5). In addition it has to be noticed that in regard to the tangential stress, only dry friction has been considered. The tangential stresses required for the subsequent analytical procedure does not follow directly from the tangential force, it is rather to be thought of as leading to the stress response. The stresses and displacements are thus iteratively related to one another so that, collectively, the conditions at the boundaries are met. Working backwards, the tangential forces are determined by integrating the tangential stresses.

(A mathematical exposition intervenes.)

Since the relationship between surface stresses and surface displacements is linear, the total stress and total displacement is determined by addition. The stresses in question can be approximated to any desired accuracy in a finite interval by using polynomials. The substitution of these polynomials in the equation relating stress to displacement, makes the evaluation of the displacement possible and hence

overall displacement is determined by integration over all the contact surface elements. Following Galin, this result is then formulated as a polynomial. Between the coefficients of the stress polynomial and the displacement differences there is then necessarily a functional relationship.

(The mathematical development relates the boundary conditions, the stresses and the resulting creep.)

2.3 CREEP THEORY (FREDERICK)

In contrast to Kalker, Frederick basis his calculations on a velocity and pressure dependent creep coefficient. By a method of approximations, he determines a boundary creep of up to 1% after which no locked region exists in the contact region. This fact enables him to deny, in general, the existence of a locked region.

Frederick calculates the coefficient $\mu(v,p)$ as follows:

$$\mu(v,p) = \mu(v,p_o) \quad \frac{470/p^{0.9} + 0.08}{470/p_o^{0.9} + 0.08}$$

where v = creep velocity
p = normal stress
p_o = 6 500 kp/cm^2

This relationship is shown in Figure 6. This equation enables him to appreciably simplify the statement for the tangential stress. To determine the contact region, the normal stress distribution and the creep velocity, Frederick uses the same statements as does Kalker but however without reference to spin, so that his equations are somewhat simpler than Kalker's. He then determines the local creep velocity by multiplying the derived coefficients by

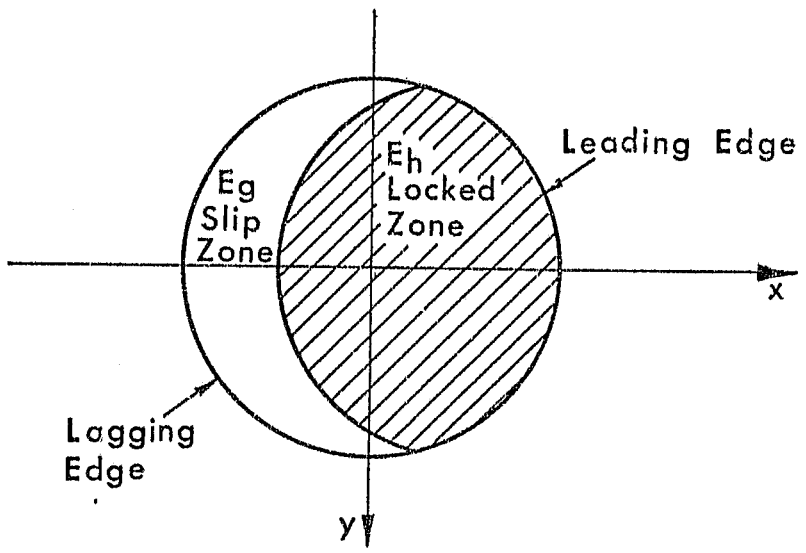

Figure 5 - Locked and Slip Zones with Circular Contact Surfaces

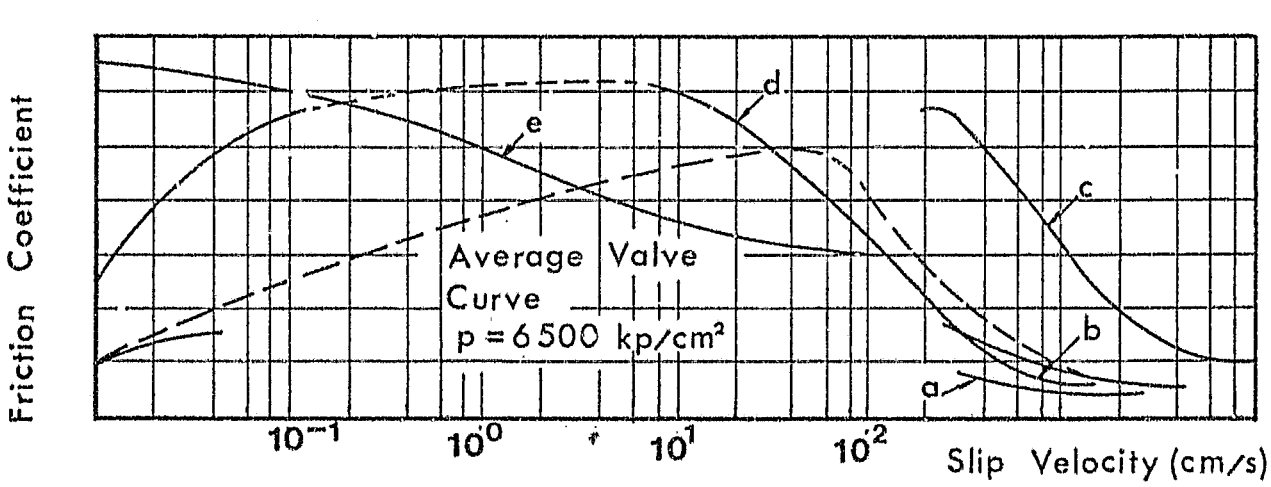

Figure 6 - Coefficient of Dry Friction with Different Slip Velocities as given by Various Researchers

(a) Braked Wheel and Rails 15 M_T Axle Loading (Meltzgur)
(b) Braked Wheel and Rails 9 M_T Axle Loading (Meltzgur)
(c) Steel on Steel, Surface Pressure 4.2 kg/cm² (Seregin)
(d) Steel on Steel (Kroegelskij)
(e) Steel on Steel (Rabinovicz)

the rolling velocity.

In contrast to Kalker, who uses the tangential stress to initiate his calculations, Frederick proceeds from the normal stress distribution derived by Hertz and finds the creep velocities in relation to the coordinate axis origin. Using the value for $\mu(v,p)$ the creep coefficient and the normal stress distribution, it is possible to calculate the tangential stresses. Following Love, the displacement differences are then determined. With the related localized creep coefficients which have been calculated, the tangential stresses can be calculated afresh. This procedure is continued until the difference between two successive iteration steps has been reduced to some prescribed minimum. From the tangential stresses derived in this manner, the tangential forces over the contact surface can be found. Frederick uses a grid pattern established over the contact area for his numerical calculations.

3. CHOICE OF METHOD FOR ESTABLISHING THE FRICTION LAWS WHICH SATISFY THE RESEARCH REQUIREMENTS

3.1 A Comparison between the two theories and the choice of a theory

In addition to the neglect of spin by Frederick, the essential difference in the two theories is the hypothesis relating to the contact surface. A discussion as to which theory corresponds sufficiently closely to reality can only be found by examining the available experimental test results.

The question as to the existence of a locked region and a creep region was firmly established by Ollerton. In his experiments, he rolled a black rubber toroid over a glass

plate coated with carbenadium. Photographs taken by him for various values of constant spin, longitudinal and transverse creep clearly demonstrate that the contact surface is separated into two distinct regions. The basis for this deduction is that the smudged zone in the locked region is made evident by an increased reflection of light. Figure 7 shows that there is wide agreement between the experimental results obtained by Ollerton and the theoretical predictions made by Kalker.

Following the theory of Kalker, the limiting frictional force occurs when the locked region vanishes. He has shown this to be the case when the creep reaches about 1% which agrees with the estimated calculated boundary creep as estimated by Frederick. In contrast to this, according to the calculations made by Frederick, the limiting frictional force is reached for creep coefficients of 40% and over for creep velocities of less than 1 Km/h. This is contradicted by practically all the experimental evidence (as evidence for this the results of Lipsius and Weber can be quoted).

If the curves shown in Figure 6 are examined, the following deductions are possible:

1. All the curves show a marked decreasing tendency for creep speeds in excess of 1 Km/h
2. No single tendency is evidenced for creep velocities of less than 1 Km/h and it would appear that a constant friction coefficient is more likely than the average value image proposed by Frederick.

In addition, the theory of Kalker is supported by the tests carried out by Krause, who found that the limiting friction coefficient was independent of the creep coefficients providing these were small. This result is explicable only if the existence of a locked region is admitted.

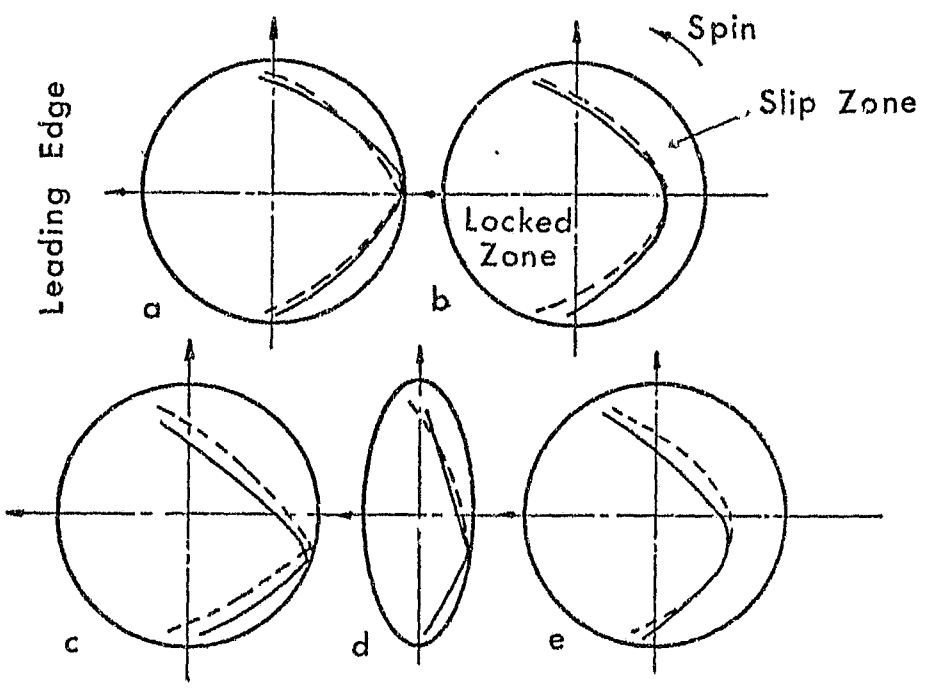

Figure 7 - Comparison Between Calculated and Measured Locked and Slip Zones

(a) Rolling with Spin

(b) Rolling with Spin and Transverse Slip

(c) Rolling with Spin and Longitudinal Force (a:b = 1)

(d) Rolling with Spin and Longitudinal Force (a:b = 0.4)

(e) Rolling with Spin, Transverse Slip and Longitudinal Force

Pure sliding in the contact area occurs not only in the case of mixed friction as well as fluid friction but is also the case in dry friction reached after limiting friction has been attained. In all these cases, the transmitted force between the wheel and the rail can be made known by the equations established by Frederick.

After comparing the two theories, it would appear desirable to give preference to the theory developed by Kalker. For the simulation, it is now necessary to calculate the tangential forces in the contact area for every time interval. The time required to calculate any measured point for a fourth order polynomial and 100 points in every revision takes 87 seconds so that it is readily understood that such a scale for the simulation is not possible. One therefore goes to a method of calculation which, while retaining the hypothesis made by Kalker, needs less calculating time. This is offered by the simplified theory of Kalker which reduces the calculating time by a factor of one hundred.

3.2 and 3.2.1 describe the simplified theory of Kalker's and a linearized theory. In the latter case it is pointed out that great difficulties exist in the determination of the locked and creep regions. De Pater proposed therefore, to meet this difficulty, that where the extent of creep was small, its influence could be neglected and this has been worked out by Kalker in his dissertation. This is then explained and in section 3.2.2 the non linear theory allowing for creep and spin is detailed. In the final paragraph it is concluded that a comparison of the results produced by calculation showed the deviation in the approximate theory as compared with the exact theory would amount to a maximum of 25%.

4. RECAPITULATION AND CRITICAL EVALUATION OF THE METHOD CHOSEN

As carried out in the previous section, both the sliding and the locked region theory have physical justification. For small magnitudes of creep, which are meaningful within the framework of the rail-wheel research resources which were theoretically available, then the force transmission between the wheel and the rail is determined by the locked region theory. Since the computation time required for the simulation is a significant cost factor, it is unavoidable that in calculating the transmitted force the simplified theory of Kalker is resorted to even though in the non linear region an error of a maximum of 25% can occur.

4.1 PHYSICAL FACTUAL SITUATION

The simplified and the exact theory of Kalker emerge from the same physical requirements. Because of the statement of approximation relating displacement and stress (in which the relationship is assumed to be linear), the simplified form then only approximates to the real situation in which it is assumed that both the bodies have the same elastic constants.

C Th Muller has however found that the hardness of both wheel and rail increases towards the running surfaces. This particular relationship was confirmed by Krause who found that the metal crystal structure was elongated in the direction of rolling and in the rolling surface. A layer which has a thickness of from 0.2 mm to 0.4 mm then exists in which the physical properties change. The running surface has as a consequence different elastic constants as compared with the remaining material which must lead to deviations from the theoretically derived values of Kalker. This affect is nevertheless allowed for in the modified assumptions

made by Kalker and Krettek. If the calculated frictional force coefficient is related to the limiting friction, the maximum creep coefficient is eliminated and a normalized friction force - creep response is obtained. The creep coefficient remains thus unknown in the caluclation of the transmitted frictional force. It should be noticed that the affects of the inertial forces brought about by the acceleration of the mass elements in the contact surface have been neglected.

4.2 COMPARISON WITH MEASURED VALUES

The normalization described in section 4.1 is required if the theoretically derived force transmitted curves are to be compared with those derived by experiment. It is required in the application of the theory of Kalker to recognise that the test bodies and the real rail-wheel system have different geometrical shapes. If all the frictional force coefficients are to be related to the wheel-rail system, the radii of the test bodies have to be adjusted accordingly. This conversion was carried out at the Institute for Mechanical Conveyance and Railway Vehicles in consultation with Krettek.

The comparison extends to the frictional force curves based on measurements by Muller (wheels on rails) and to the tests carried out by the institution referred to on their roll test stand I (rolls on rolls). In order to compare the calculated curves, based on the theory of Kalker, allowance has been made for the separate cross sectional area relationships as well as for the different G and E values. (Both for the non-deformed as well as for the plastically deformed condition.)

Figure 8 shows the satisfactory agreement between the theoretically derived and the experimentally based curves. According to Krettek, it is now possible to relate all the values to the wheel-rail system of the test results obtained on the roll test stand by using Kalker's theory. Figures 9* and 10* show the comparison of the various values where Figure 9 is for the underformed and Figure 10 for the deformed material. It has again been possible to establish satisfactory agreement between the various results. The maximum deviation between the test results and the theoretically calculated values is between 11 and 12% and decreases with smaller force transmission coefficients.

5. CONFIRMATION OF THE LOCKED AREA THEORY BY FURTHER EXPERIMENTATION

5.1 OUTSTANDING TESTS

From what has been said it is apparent that the frictional force - creep process has been satisfactorily explained to a considerable degree. There has not been experimental verification of the relationship between simultaneous longitudinal, transverse and circular creep. Unknown is also the relationships determining the creep coefficient. All research so far has shown that it is dependent on a series of parameters. These must be investigated and the functional relationship between the creep coefficient and the related parameters determined. Such parameters are: creep velocity, rolling speed, metallic surface properties, plastic deformation, environmental variations and conditions in the contact area (dry, lubricated). Equally unknown are the elastic constants for the deformed running surfaces.

---

* Not given in this translation

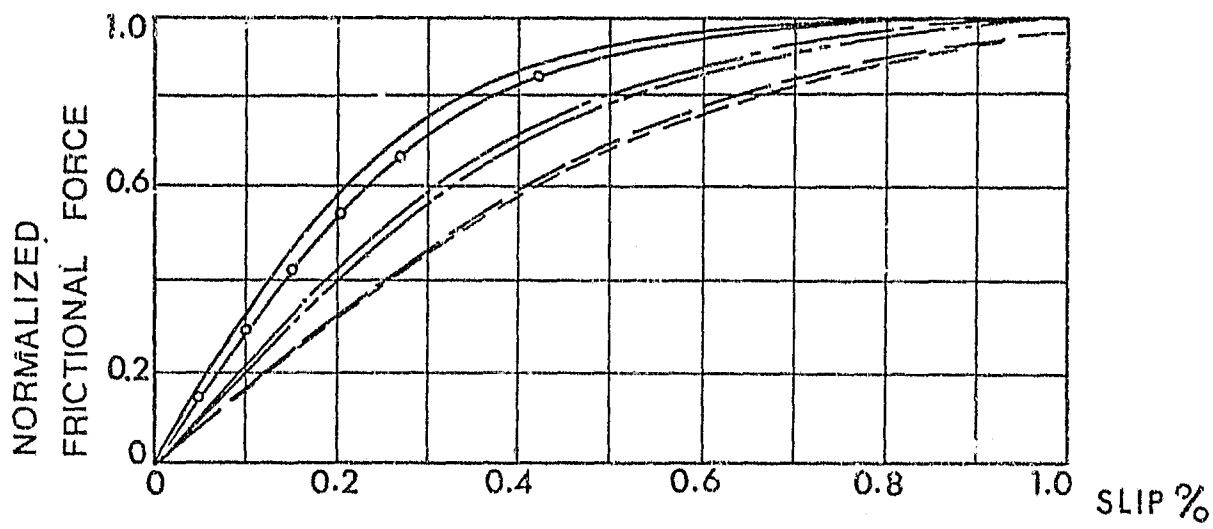

FIGURE 8

WHEEL-RAIL SYSTEM —o———o— Theoretical Values (Kalker)
——— Experimental Values (C.Th.Muller)

ROLL-ROLL SYSTEM —— - ——·— Theoretical Values (Kalker)
(No Plastic Deformation) —·—·— Experimental Values (Krause)

ROLL-ROLL SYSTEM — — — Theoretical Values (Kalker)
(Plastically Deformed) - - - - - Experimental Values (Krause)

Int. J. Solids Structures, 1965, Vol. 1, pp. 319 to 341. Pergamon Press Ltd. Printed in Great Britain

THE DYNAMIC STABILITY OF RAILWAY VEHICLE WHEELSETS AND BOGIES HAVING PROFILED WHEELS

A. H. WICKENS

British Rail Research Department, Derby

Abstract—The dynamic instability of railway vehicle bogies and wheelsets is caused by the combined action of the conicity of the wheels and the creep forces acting between the wheels and rails. In this paper, the instability is investigated in the important case where the wheels are profiled rather than purely conical. Equations of motion are formulated and stability criteria obtained which indicate the effect of varying the various parameters of the system. The nature of the motion at the critical speed is investigated and the mode of energy conversion between the forward motion of the vehicle and the lateral motion of the bogie or wheelset is explained.

NOTATION

$2a$	length of contact area in direction of rolling
a_1, a_2	relative amplitudes of generalized coordinates ϕ_1 and ϕ_2
$2b$	length of contact area transverse to direction of rolling
C	moment of inertia in yaw of wheelset
d	length, defined in Fig. 1
d_1, d_2	suspension viscous damping coefficients in longitudinal and lateral directions
f, f'	longitudinal and lateral creep coefficients
F	dissipation function
G	modulus of rigidity
j	$= C/ml^2$
J	moment of inertia of bogie divided by ml^2
k_1, k_2	suspension elastic stiffness coefficients in longitudinal and lateral directions
l	length, defined in Fig. 1
m	mass of wheelset
M	tractive torque
N, N'	normal reactions at contact points
p_i	coefficients in characteristic equation
P	tractive force
q_1	lateral displacement of wheelset or bogie
q_2	yaw of wheelset or bogie
Q_1	lateral force exerted by rails on wheelset
Q_2	yawing moment exerted by rails on wheelset
r_0	wheel tread circle radius, wheelset in central position
r, r'	radii of tread circles, wheelset displaced laterally
R	radius of curvature of wheel tread
R	radius of curvature of rail head
s	$= \dfrac{l}{V_0}\dfrac{\mathrm{d}}{\mathrm{d}t}$
t	time
T	kinetic energy
v	$= V/V_0$
v_{c1}, v_{c2}	non-dimensional critical speeds
V	forward speed of vehicle; potential energy
V_0	reference speed
W	axle-load

α	$= 2l/r_0$
β	length, defined in Fig. 1
γ, γ'	longitudinal and lateral creepages
γ	mass of bogie divided by mass of wheelset
δ, δ'	angle between contact plane and horizontal at contact points
δ_0	angle between contact plane and horizontal, wheelset in central position
ε	defined by equation (3)
$\varepsilon_1, \varepsilon_2, \varepsilon_3$	non-dimensional stiffness coefficients
$\varepsilon_{11}, \varepsilon_{12}$	non-dimensional damping coefficients
λ	effective conicity
λ_0	$= n_0 - w$, root of characteristic equation
θ	phase angle
μ, μ'	non-dimensional creep coefficients
ν	$= v/V_0$
ϕ_2	$= q_2 l$
ϕ_3	$= q_3$
Φ, Ψ_1	functions of $(a\ b)$ involved in calculation of creep coefficients
ω	circular frequency
Ω	$= V/V_0 r_0$

INTRODUCTION

AT CERTAIN forward speeds, some railway vehicles experience sustained oscillations in the lateral plane. These oscillations arise because of the dynamic instability of these vehicles caused by interaction between the conicity of the wheels, the forces acting between the wheels and the rails and the action of the suspension. Railway vehicles were originally provided with coned wheels in order to obtain a measure of static stability, but as wheel treads rapidly wear with use, wheels which commence life with conical treads come to possess concave treads which possess curvature in the transverse direction. The behaviour of a vehicle with profiled wheels of this type is significantly different from that of a vehicle with coned wheels, and this paper presents a general theory of the stability of the small oscillations of elastically restrained wheelsets (a wheelset consisting of two wheels mounted on a rigid, common axle) and bogies having profiled wheels.

The system considered consists of a single wheelset or bogie (Fig. 1) connected by means of an elastic suspension to a vehicle body which is assumed to move forward at constant velocity with negligible lateral motion. The suspension possesses flexibility in the longitudinal and lateral directions. The bogie consists of two wheelsets mounted, without lateral or longitudinal flexibility, in a rigid frame. The neglect of the lateral motions of the vehicle body can be justified in general terms on the basis that the body has a much greater mass than a wheelset or bogie and that the instability discussed here occurs at frequencies which are much higher than the natural frequencies of the body oscillating on the suspension. A more specific justification can be given by considering the stability of a complete vehicle with appropriate body freedoms; this will be done in a sequel to this paper.

It is well known that an elastic structure which is subject to non-conservative forces may become dynamically unstable under certain conditions of loading. Apart from the instabilities of other wheeled vehicles, such as shimmy of automobiles, examples of elastic systems of this kind are provided by structures loaded by aerodynamic or hydrodynamic forces, rotating shafts and servo-mechanisms with structural feedback; the nature of the instabilities of systems of this type has been discussed by Bolotin [1]. In the system discussed here the non-conservative forces arise from the phenomenon of creep. When elastic bodies roll together, contact takes place over an area which can be

determined by the theory of Hertz. It has been found that a tangential force transmitted across the contact area will cause a relative velocity, or creep, of one surface relative to the other. Provided that the tangential force is less than about one third of that necessary to produce sliding of one body over the other, the creep velocity is proportional to the tangential force. Creep arises because, in the contact area, there is a region of adhesion and a region of slipping in which the tangential traction is equal to the limiting friction. The creep velocity is consistent with the difference in the elastic strains between the two bodies in the region of adhesion. As the magnitude of the tangential force increases, the region of slipping occupies a larger proportion of the contact area, until sliding occurs as the tangential force equals the limiting friction. For small values of the creep velocity, slipping is confined to the trailing edge of the contact area and the phenomenon is independent of the coefficient of friction, being governed only by the elastic strain distribution in the vicinity of the contact area.

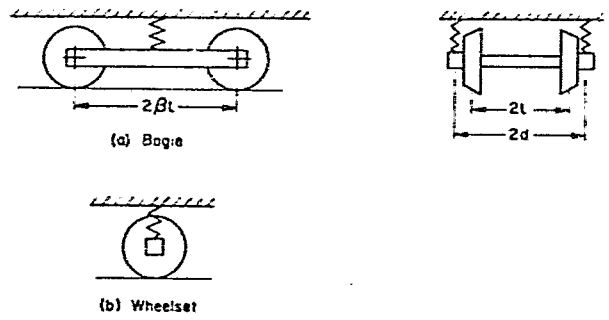

FIG. 1. Elastically restrained wheelset and bogie.

Carter [2] recognized the importance of the phenomenon of creep in the lateral dynamics of railway vehicles, and considered the stability of various configurations of locomotives [3], indicating the existence of critical speeds separating regions of stable and unstable motions. Previously, a theoretical analysis of the kinematic oscillation of a slowly rolling wheelset with coned wheels had been given by Klingel [4]. The stability of locomotives was also considered by Rocard [5], and a discussion of stability using the concept of energy balance was given by Cain [6]. Up to this time, only conical wheels had been considered but Davies [7] and Davies and Cook [8] investigated the motions of wheelsets experimentally and theoretically and indicated the importance of the wheel and rail profiles. The effect of wear of the wheel tread on the kinematic oscillation was discussed by Heumann [9]. For profiled wheels, the lateral component of the change in the normal reactions between wheel and rail as the wheelset is displaced is proportional to the lateral displacement. This effect was included in studies made by de Possel and Beautefoy [10] and by Müller [11]. The stability of a rigid trolley with coned wheels has been considered by Brann [12] and the stability of a complete vehicle with coned wheels by Matsudeira [13]. Certain non-linear aspects of the lateral dynamics of railway vehicles have been considered by de Pater and Katz [14].

EQUATIONS OF MOTION OF THE ELASTICALLY RESTRAINED WHEELSET

A wheelset which is moving along the track at constant speed has two degrees of freedom, and appropriate generalized coordinates are q_1, the lateral displacement of the centre of mass of the wheelset, and q_2 the angle of yaw of the wheelset. Local deflections of the wheelsets and rails at the points of contact will be neglected in the formulation of the equations of motions, which are

$$\begin{aligned} m\ddot{q}_1+2d_2\dot{q}_1+2k_2q_1 &= Q_1, \\ C\ddot{q}_2+2d^2d_1\dot{q}_2+2d^2k_1q_2 &= Q_2. \end{aligned} \tag{1}$$

where the generalized forces Q_1 and Q_2 represent the forces acting between the wheels and the rails. m is the mass of the wheelset, C the moment of inertia in yaw, k_1 and k_2 represent the suspension stiffnesses in the longitudinal and lateral directions and d_1 and d_2 represent the corresponding suspension dampings.

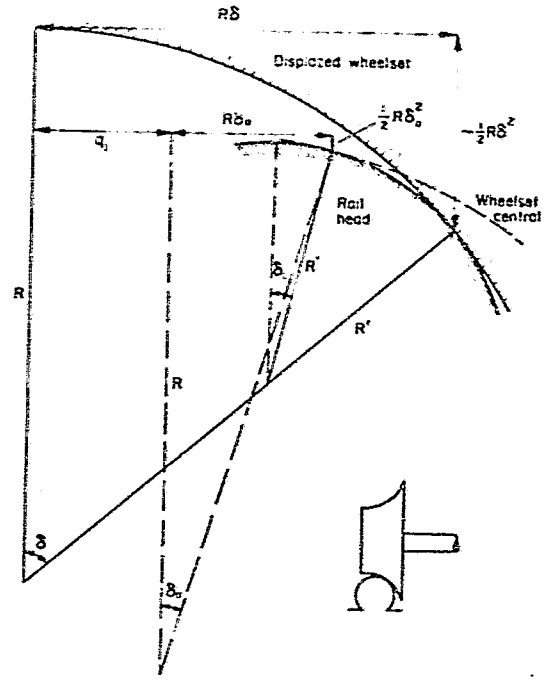

FIG. 2. Geometry of wheel and rail contact.

It will be assumed throughout the analysis that the angle made by the contact plane with the horizontal, δ_0, at each of the contact points when the wheelset is in the centre position is a small quantity of the same order as the generalized displacements, so that for the small displacements considered here, products of δ_0 with q_1 or q_2 and their

derivatives are negligible. The angle of roll of the wheelset as it is displaced laterally is then a second order quantity, and gyroscopic forces may be omitted from equations (1).

When the wheels are in the central position on the track, the tread circles of both wheels of the wheelset have the same radius r_0. When the wheelset is displaced laterally, contact occurs at new points (Fig. 2) and the angles made by the contact planes at these points are denoted by δ and δ' respectively, and the radii of the tread circles become r and r'. If R is the radius of curvature of the wheel tread and R' is the radius of curvature of the rail head, then for small displacements reference to Fig. 2 shows that

$$q_1+R\delta_0-R'\delta_0+R'\delta = R\delta,$$

or

$$\delta-\delta_0 = q_1(R-R'),$$

so that

$$\delta = \delta_0+\frac{\varepsilon q_1}{l}, \tag{2a}$$

where

$$\varepsilon = l/(R-R'). \tag{3}$$

Similarly

$$\delta' = \delta_0-\frac{\varepsilon q_1}{l}. \tag{2b}$$

Also from Fig. 2 it follows that

$$\begin{aligned} r-r_0 &= \frac{R}{2}(\delta^2-\delta_0^2) \\ &= \frac{R}{2}(\delta-\delta_0)(\delta+\delta_0) \\ &= R(\delta-\delta_0)\delta_0 \quad \text{approximately,} \\ &= R\varepsilon\delta_0 q_1/l. \end{aligned}$$

Thus

$$r = r_0+\lambda q_1, \tag{4a}$$

where

$$\lambda = R\delta_0/(R-R'). \tag{5}$$

Similarly,

$$r' = r_0-\lambda q_1. \tag{4b}$$

The parameter λ will be termed the effective conicity, for if the wheels were conical λ would be equal to the cone angle. Equation (5) is due to Heumann [9]; equations (3) and (5) were also derived by de Pater [15].

The normal reactions at the contact points, N and N', are given by

$$N = -\frac{1}{2l}\left(mr_0\ddot{q}_1 + 2d_2r_0\dot{q}_1 + 2k_2r_0q_1 - Wl\right),$$

$$N' = \frac{1}{2l}\left(mr_0\ddot{q}_1 + 2d_2r_0\dot{q}_1 + 2k_2r_0q_1 + Wl\right),$$

where W is the axle load. The lateral resultant of these normal reactions is

$$N'\delta' - N\delta$$
$$= -We q_1/l$$

representing a restoring force, as is obvious on physical grounds.

The forces acting in the contact plane arise from the phenomenon of creep and will be assumed to consist of a longitudinal and a lateral component. The longitudinal force acting on the wheel can be expressed as $-f\gamma$ where f is the longitudinal creep coefficient and γ is the longitudinal creepage, defined by Carter [2] to be

$$\gamma = \frac{\text{actual forward displacement} - \text{pure rolling forward displacement}}{\text{forward displacement due to rolling}}.$$

Similarly, the lateral force acting on the wheel can be expressed as $-f'\gamma'$ where f' is the lateral creep coefficient and γ' is the lateral creepage

$$\gamma' = \frac{\text{actual lateral displacement} - \text{pure rolling lateral displacement}}{\text{forward displacement due to rolling}}.$$

The relationship between the creepage and the creep forces has been investigated for a variety of practical situations. Carter [16] gave a solution to the creep problem for the two-dimensional case of two long cylinders, pressed together by a normal force, and transmitting a tangential force across the contact strip. Similar results were obtained by Poritsky [17], and in the discussion of [17], Cain [18] pointed out that the region of adhesion must lie at the leading edge of the contact area. A three-dimensional case was solved approximately by Johnson [19] who considered an elastic sphere rolling on an elastic plane. This solution was based on the assumption that the area of adhesion is circular and tangential to the area of contact (which is also circular) at the leading edge. Reasonably good agreement with experiment was obtained. The influence of spin about an axis normal to the contact area has also been studied by Johnson [20]. De Pater [21] has also investigated the case where the contact area is circular, and derived solutions for both small and large creepages, without making assumptions about the shape of the area of adhesion. However, this analysis was confined to the case where Poisson's ratio was zero. Kalker [22] has given a complete analytical treatment for the case in which Poisson's ratio is not zero. The agreement between these theoretical results and the experimental results of Johnson [19] is very good. The general case where the contact area is elliptical has been considered by Haines and Ollerton [23] who confine their attention to creep in the direction of motion and assume that Carter's two-dimensional stress distribution holds in strips parallel to the direction of motion. A general theory for the elliptical contact area, based on similar assumptions to those made in [19], has

been developed by Vermeulen and Johnson [24], yielding the relationship between creepages and tangential forces for arbitrary values of the ratio of the semi-axes of the contact area.

According to the solution given by Vermeulen and Johnson [24] the creep functions are given by the expressions

$$f = G\pi ab\,\Phi,$$

$$f' = G\pi ab\,\psi_1,$$

where G is the modulus of rigidity, $2a$ is the length of the contact area in the direction of rolling and $2b$ is the length of the contact area transverse to the direction of rolling. The functions Φ and ψ_1 depend on a/b and Poisson's ratio only, and have been derived and plotted in [24]. The dimensions of the contact area are obtained from the relations due to Hertz, and depend on the relative curvatures of wheel and rail and the normal reaction N. From [25],

$$\left(\frac{a}{m}\right)^3 = \left(\frac{b}{n}\right)^3 = \frac{3(1-\sigma)N}{2\left(\frac{1}{R} + \frac{1}{R'} + \frac{1}{r_0}\right)G}$$

where m, n are constants dependent on the curvatures, and σ is Poisson's ratio. Values for m, n are tabulated in [25]. The creep coefficients are proportional to $N^{2/3}$, and in the case where the contact area is circular, $a/b = 1$, and

$$\Phi = \pi(4-3\sigma)/16,$$

$$\psi_1 = \pi(4-\sigma)/16.$$

It will be assumed in the present analysis that the effect of variation of the normal reaction due to the motion of the wheelset has a negligible effect on the value of the creep coefficients.

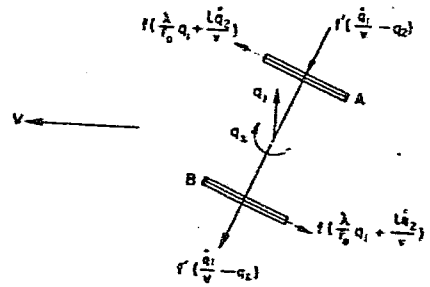

FIG. 3. Creep forces acting on wheelset.

A forward motion of the wheelset in a small interval of time results in the following displacements at the wheel tread in the longitudinal and lateral directions respectively, for wheel A (Fig. 3)

$$V\,dt - l\,dq_2, \qquad dq_1,$$

and for wheel B

$$V\,dt+l\,dq_2, \qquad dq_1.$$

Because δ_0 is considered small, the difference between the lateral displacement of wheelset at the centre of mass and at the treads due to tilting of the wheelset is neglected. The corresponding components of rolling displacements are, for wheel A

$$(r_0+\lambda q_1)V\,dt, \qquad q_2V\,dt,$$

and for wheel B

$$(r_0-\lambda q_1)V\,dt, \qquad q_2V\,dt.$$

It follows that the creepages are, for wheel A

$$\gamma = -\frac{\lambda}{r_0}q_1-\frac{l}{V}\dot{q}_2, \tag{6}$$

$$\gamma' = \frac{\dot{q}_1}{V}-q_2,$$

and for wheel B

$$\gamma = \frac{\lambda}{r_0}q_1+\frac{l}{V}\dot{q}_2, \tag{7}$$

$$\gamma' = \frac{\dot{q}_1}{V}-q_2.$$

The generalized forces Q_1 and Q_2 can now be written down in the form

$$Q_1 = -\frac{2f'\dot{q}_1}{V}+2f'q_2-W\varepsilon\frac{q_1}{l}, \tag{8}$$

$$Q_2 = -\frac{2fl^2\dot{q}_2}{V}-\frac{2f\lambda l}{r_0}q_1.$$

Substituting from equations (8) into equations (1) and defining the following non-dimensional quantities

$$\mu = 2fl/mV_0^2, \qquad \mu' = 2f'l/mV_0^2,$$

$$\alpha = \lambda l/r_0, \qquad v = V/V_0, \qquad s = \frac{l}{V_0}\frac{d}{dt},$$

$$j = C/ml^2, \qquad \zeta_1 = 2d_1d/mV_0, \qquad \zeta_2 = 2d_2l/mV_0,$$

$$\varepsilon_1 = 2k_1d^2/mV_0^2, \qquad \varepsilon_2 = 2k_2l^2/mV_0^2, \qquad \bar{\varepsilon}_2 = W\varepsilon l/mV_0^2,$$

$$\phi_1 = q_1/l, \qquad \phi_2 = q_2, \qquad \bar{\varepsilon}_2 = \varepsilon_2+\bar{\varepsilon}_2,$$

where V_0 is a reference velocity, the equations of motion take the form

$$\left[s^2+\left(\frac{\mu'}{v}+\zeta_2\right)s+\bar{\varepsilon}_2\right]\phi_1-\mu'\phi_2 = 0, \tag{9}$$

$$\mu\alpha\phi_1+\left[js^2+\left(\frac{\mu}{v}+\zeta_1\right)s+\varepsilon_1\right]\phi_2 = 0.$$

The non-conservative nature of the system is indicated by the assymmetry of the coupling terms due to creep and conicity. It is due to this property that dynamic instability can occur.

Some typical values are

$$r_0 = 1{\cdot}75\text{ ft}, \qquad l = 2{\cdot}5\text{ ft}, \qquad d = 3{\cdot}25\text{ ft},$$

$$m = 90\text{ slugs}, \qquad C = 360\text{ slugs ft}^2, \qquad W = 9300\text{ lb},$$

$$k_1 = k_2 = 5000\text{ lb/ft}, \qquad f = f' = 3\times10^6\text{ lb},$$

$$R' = 0{\cdot}690\text{ ft}, \qquad R = 0{\cdot}787\text{ ft}, \qquad \delta_0 = 0{\cdot}05,$$

and taking the reference velocity $V_0 = 100$ ft/sec it follows that

$$\mu = \mu' = 16{\cdot}7 \qquad \alpha = 0{\cdot}571, \qquad j = 0{\cdot}640,$$

$$\varepsilon_1 = 0{\cdot}1176, \qquad \varepsilon_2 = 0{\cdot}0694, \qquad \bar{\varepsilon}_2 = 0{\cdot}6562.$$

These numerical values will be used to illustrate the theory as it is developed.

KINEMATIC OSCILLATIONS OF WHEELSETS

Before considering the stability of the elastically restrained wheelset it is useful to consider the behaviour of an unrestrained wheelset in motion at a low forward speed. The theory appears to have been first given by Klingel [4]; it is also discussed by Carter [2].

As the wheelset is unrestrained, the elastic suspension stiffnesses will be zero. To obtain the solution of Carter it is also necessary to neglect the gravitational stiffness terms which were not included in Carter's analysis. Also neglecting the inertia terms, the equations of motion reduce to

$$\frac{\mu's}{v}\phi_1-\mu'\phi_2 = 0,$$

$$-\phi_1+\frac{\mu s}{v}\phi_2 = 0.$$

Elimination of ϕ_1 and ϕ_2 yields

$$s^2 = -\alpha v^2$$

indicating that the motion has a single undamped oscillatory constituent with frequency ν given by

$$\nu^2 = \alpha v^2. \tag{10}$$

In dimensional terms, the freqnency is

$$\omega = V\sqrt{\frac{\lambda}{r_0l}}$$

and is therefore proportional to the forward speed of the wheelset.

J. Sound Vib. (1966) 4, (1), 18–32

SOME ASPECTS OF THE HUNTING OF A RAILWAY AXLE

R. P. Brann

Department of Mechanical Engineering, University College London, London, W.C.1

(Received 16 October 1965)

Equations of motion are derived to describe the hunting mode of a railway axle running at constant velocity along straight track. It is assumed that the wheel and rail-head profiles take some arbitrary shape. This shape gives rise to non-linearities in the equations.

The equations are first linearized, and approximate expressions derived for the frequency of the oscillation and conditions of stability. Asymptotic stability for all initial conditions of the non-linear system is then considered in the manner of Aiserman, and the equations are examined for stable limit-cycles by applying the first approximations of Kryloff and Bogoliuboff. It is shown that, when running at low velocities, the axle will execute limit-cycle oscillations even though the wheel's flanges do not contact the rails. Small increases in velocity, however, quickly result in flange contact.

1. INTRODUCTION

The problem of bogie-hunting has been the subject of many investigations although it is still essentially unsolved in any but the simplest of idealizations. The system does not lend itself readily to linear analysis, but linear equations of motion can be derived (1) from which frequency expressions and conditions for stability may be extracted. If the linear equations are relevant to a bogie running on track, they can only be so when the hunting motions are infinitesimal: that is, they can only define the onset of hunting. When the motions become large, such factors as flange/rail contact and overall wheel skid introduce non-linearities which limit the oscillation.

When a wheel has been in service for some time, the straight conical profile of the tyre wears to a concave form. This concavity blends into the flange radius at the throat of the wheel. The profile of a wheel is therefore a continuous curve and when the axle as a whole hunts upon the track, the wheel/rail contact points move along two such curves. When the lateral deflection of the axle becomes large, one contact point moves well into a flange radius and it is conceivable that a large lateral force could be set up which would tend to restore the system to its equilibrium configuration. It is reasonable, therefore, to presume that under certain conditions the system would execute a stable limit cycle even though the wheel's flange would never come into immediate contact with the rails. It is the object of this work to examine the single-axle system theoretically and find conditions under which such a limit cycle would prevail, and its subsequent stability.

De Pater (2) used the method of Kryloff and Bogoliuboff to examine the steady-state motion of a railway bogie. He assumed that the wheels were cylindrical and he theoretically observed how periodic flange/rail impact forces induced the system into a limit cycle. Johnsson (3) also investigated the motion in the large of railway vehicles. He used an analogue computer and examined the effects of non-linearities in the suspension systems, such as "hard" springs. However, there appears to be no study in the literature of the behaviour of the system when it is in a state of transition between running on straight cones (which is applicable to linear theory) and oscillating under the influence of hard flange/rail contact. It seems probable that steady-state hunting would occur when such a transition condition is in operation.

2. EQUATIONS OF MOTION

2.1. WHEEL/RAIL INTERACTION FORCES

It is to be assumed in everything that follows that the tangential forces acting upon a wheel by the rail which contacts it obey the linear laws of creepage. If a wheel rolls perfectly upon a rail, the wheel/rail contact point is instantaneously stationary. When imperfect rolling occurs, however, the contact point migrates (or creeps) over the rail. The contact force which acts in the plane of the rail as a result of this creepage is assumed to be proportional to the velocity of the creep as defined by Carter (4). The constant of proportionality is f/V, where f is a constant which depends upon the elastic parameters of the wheel and track materials and V is the forward velocity of the wheel. For convenience, the creep velocity vector is written in terms of two orthogonal components: one in the plane of the wheel (longitudinal) and the other at right angles to the wheel (lateral). The constant f is assumed to be equal for both components.

Finally, it should be stated that the phenomenon of creepage (and hence the linearity of this aspect of the system) prevails only so long as the ratio of normal wheel load to tangential force remains substantially less than the coefficient of friction of the wheel and rail materials. This is a condition which must be assumed to exist in the subsequent analysis.

2.2. CREEP VELOCITIES

Consider the railway axle rolling on a straight rigid track as in Figure 1. The wheel-tyre and rail-head profiles take some arbitrary shapes as shown in the figure. As yet these shapes will remain unspecified; all that will be said of them is that, when the system is in the static equilibrium configuration, they are such that geometric symmetry exists about the vertical plane through the track's centre-line, and that for all finite displacements a wheel contacts its rail at one point only.

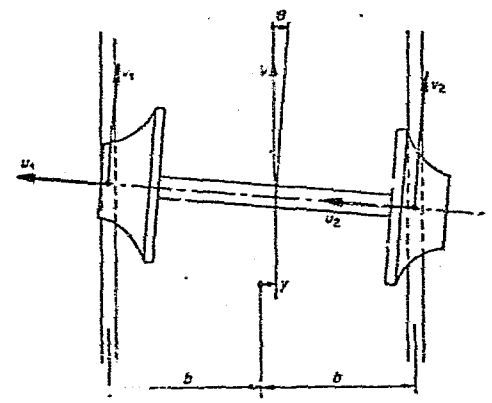

Figure 1. Axle rolling on track.

The axle is rolling at constant velocity V along the track and the two generalized co-ordinates which define its position and orientation are y and θ as illustrated in Figure 1. When both of these are zero, the radius of contact of each wheel is r, and the slopes of the common tangents at the wheel/rail contact points are $-\alpha$ for wheel 1 and $+\alpha$ for wheel 2. This angle is of the order of $\tan^{-1}(0{\cdot}05)$ in a real system.

The lateral creep velocities are to be considered first. Despite the arbitrary shapes of the wheel and rail-head profiles, it is assumed that the absolute velocities of the two contact points along both wheels are equal to $\dot{y}$. This absolute motion (for each wheel) is comprised of a velocity component arising out of pure rolling together with a creep velocity. The first component is equal to $V\theta$, to the first order of approximation. The lateral creep velocity being sought is therefore the difference between $\dot{y}$ and $V\theta$. We therefore have

$$u_1 = \dot{y} - V\theta = u_2 = u, \tag{1}$$

where the directions of u_1 and u_2 are shown in Figure 1.

The longitudinal creep velocity of each wheel is more easily realized. It is merely the absolute instantaneous velocity of a particle on the wheel that lies "within" the contact point. The longitudinal creep velocities shown in Figure 1 are therefore given by

$$\left.\begin{aligned} v_1 &= V - \Omega r_1 + b\dot{\theta} \\ v_2 &= V - \Omega r_2 - b\dot{\theta} \end{aligned}\right\} \tag{2}$$

to the first order of approximation.†

2.3. DYNAMIC EQUILIBRIUM

Now that the creep forces have been defined, it is an easy matter to apply Newton's laws to derive the system's equations of motion. A free-body diagram of the axle arbitrarily displaced upon the track is illustrated in Figure 2. The lateral creep forces are shown as F_1 and F_2, the longitudinal creep forces as P_1 and P_2, and the normal forces as N_1 and N_2. The creep forces are given by

$$\left.\begin{aligned} F_1 &= \frac{f}{V}.u = F_2 \\ P_1 &= \frac{f}{V}.v_1, \quad P_2 = \frac{f}{V}.v_2 \end{aligned}\right\}, \tag{3}$$

while the vertical components of N_1 and N_2 are assumed to remain constant and equal to $mg/2$.

On considering dynamic equilibrium of the axle's centre of mass in the lateral direction, the equation

$$m\ddot{y} + \{(N_2' - N_1') + (F_1' + F_2')\}\cos\theta = 0 \tag{4}$$

is obtained, and expanded to

$$m\ddot{y} + \frac{mg}{2}(\tan\delta_2 - \tan\delta_1) + \frac{f}{V}u(\cos\delta_1 + \cos\delta_2) = 0 \tag{5}$$

when $\cos\theta$ is approximated to one. Now variation of the angles δ_1 and δ_2 with y clearly depends upon the wheel and rail-head profiles. Further, because of the symmetry of the undisplaced system about the vertical plane containing the track's centre-line, the term $(\tan\delta_2 - \tan\delta_1)$ must be an odd function of y: that is,

$$\tan\delta_2 - \tan\delta_1 = \sum_{s=0}^{n} e_s y^{2s+1}, \tag{6}$$

where n is any integer, and the e_s are constants. It will be noted that any contribution due to θ is neglected. The term $(\cos\delta_1 + \cos\delta_2)$, on the other hand, is not so easy to define. It is certainly not a powerful function of the lateral displacement (as is the expression in equation

† A list of symbols is given in Appendix 1.

(6)), but could remain substantially constant over a wide range of y. It will therefore be assumed that

$$\cos\delta_1 + \cos\delta_2 = k \quad (k < 2), \tag{7}$$

where k is a constant. Equation (5) is finally expanded into

$$m\ddot{y} + \frac{fk}{V}\dot{y} + \frac{mg}{2}\sum_{s=0}^{n} e_s y^{2s+1} = fk\theta, \tag{8}$$

when substitutions are made from equations (1), (6) and (7).

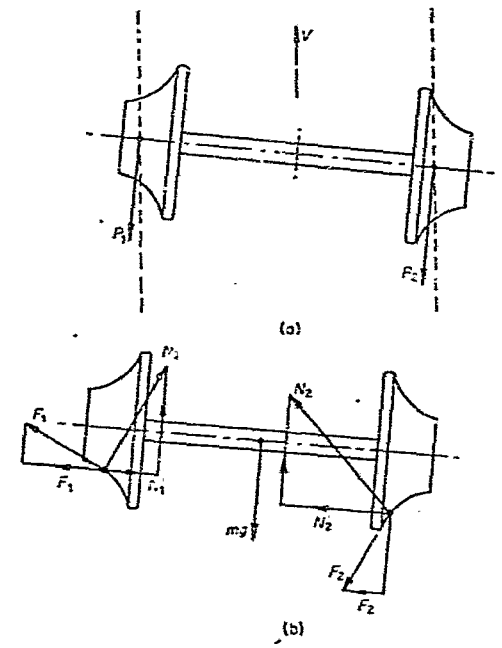

Figure 2. Free body diagram of axle. (a) Plan; (b) elevation.

Dynamic equilibrium is now considered in the direction of the angular displacement θ to give the equation

$$\mathcal{J}\ddot{\theta} + b(P_1 - P_2) = 0, \tag{9}$$

which is expanded using equations (2) and (3) to

$$\mathcal{J}\ddot{\theta} + \frac{fb^2}{V}\dot{\theta} = \frac{f\Omega}{V}(r_1 - r_2). \tag{10}$$

The term $(r_1 - r_2)$ clearly depends upon the shape of the wheel and rail-head profiles. As in the case of $(\tan\delta_2 - \tan\delta_1)$ it is an odd function of y and will be assumed to be independent of θ. The approximation will be taken further here, however, because only the first term in the power series of y will be considered.† It will be assumed that the wheels have straight conical profiles (of included angles 2α) and that the rail-heads are arcs of a circle of radius c.

† It is felt that the non-linearity associated with $(r_1 - r_2)$ is outweighed by that associated with $(\tan\delta_2 - \tan\delta_1)$.

When the axle is displaced laterally by a distance y, it can be shown that the wheel/rail contact points move distances approximately $(y+\phi c)$ axially along each wheel, where ϕ is the angle of roll of the axle. It can further be shown that

$$\phi = \alpha' \frac{y}{b}, \tag{11}$$

where $\alpha' = \alpha'(1-2\alpha c/b)$. The term (r_1-r_2) in equation (10) can therefore be written as $2\alpha(y+\phi c)$ which is simplified to

$$r_1 - r_2 = -2y\alpha'', \tag{12}$$

where $\alpha'' = \alpha(1+\alpha' c/b)$. It is also assumed that $\Omega = V/r$, so that equation (10) is finally rewritten as

$$\ddot{y} + \frac{fb^2}{V^2}\dot{\theta} = -\frac{2fb\alpha''}{r}y. \tag{13}$$

It is convenient at this stage to express the two equations of motion (equations (8) and (13)) non-dimensionally. To this end the displacement and time parameters,

$$\lambda = \frac{y}{b}, \quad \tau = \frac{V}{b}t, \tag{14}$$

are introduced and the equations rewritten as

$$\ddot{\lambda} + \frac{fbk}{V^2 m}\lambda + \frac{2b^2}{2V^2}\sum_{s=0}^{n} \epsilon_s \lambda^{2s+1} = \frac{fbk}{V^2 m}\theta, \tag{15}$$

$$\ddot{\theta} + \frac{2b^2 f}{V^2 J}\theta = -\frac{2fb^2\alpha''}{Jr}\lambda, \tag{16}$$

where

$$\epsilon_s' = \epsilon_s b^{2s+1}. \tag{17}$$

The dots shown above λ and θ now represent differentiation with respect to τ. Finally, the equations are written in the form

$$\ddot{\lambda} + \gamma\dot{\lambda} + \sum_{s=0}^{n} \epsilon_s \lambda^{2s+1} = \gamma\theta, \tag{18}$$

where

$$\ddot{\theta} + \gamma\sigma\dot{\theta} = -\gamma\sigma\beta\lambda, \tag{19}$$

$$\gamma = \frac{fbk}{V^2 m}, \tag{20}$$

$$\sigma = \frac{2mb^2}{kJ}, \tag{21}$$

$$\beta = \frac{b\alpha''}{r}, \tag{22}$$

and

$$\epsilon_s = \frac{gb\epsilon_s'}{2V^2}. \tag{23}$$

It can be seen that the two equations of motion are coupled by linear terms, and that one has a direct non-linear spring term. It is this, as we shall see, which enables the system to oscillate in a finite limit-cycle.

3. INFINITESIMAL MOTIONS

It is relevant to consider the linear system first in order to define conditions under which initial instability prevails. It is also of value to know the linear frequency of the motion since this will be used in approximating equations (18) and (19) to enable the non-linear system to be put into a more suitable form.

Linear equations are derived from equations (18) and (19) when

$$\sum_{s=0}^{n} \epsilon_s \lambda^{2s+1} \to \epsilon_0 \lambda.$$

In physical terms, this is merely an expression of the assumption that the wheels are linear cones. The system is then defined by

$$\left.\begin{aligned} \ddot{\lambda} + \gamma\dot{\lambda} + \epsilon_0\lambda &= \gamma\theta \\ \ddot{\theta} + \gamma\sigma\dot{\theta} &= -\gamma\sigma\beta\lambda \end{aligned}\right\}. \tag{24}$$

Now, as a first, somewhat gross, approximation, it is assumed that the velocity, V, and frequency of oscillation, ω, of the system are small. In such a condition it is reasonable to suppose that the axle is dominated by the tangential forces acting upon it by the track. In other words, it is assumed that the terms in equations (24) which contain γ predominate. All others are therefore neglected to yield

$$\left.\begin{aligned} \ddot{\lambda} &= \theta \\ \ddot{\theta} &= -\beta\lambda \end{aligned}\right\}. \tag{25}$$

These are solved to give

$$\left.\begin{aligned} \lambda &= \hat{\lambda}\sin(\nu\tau+\xi), \\ \theta &= \nu\hat{\lambda}\sin\left(\nu\tau+\xi+\frac{\pi}{2}\right), \end{aligned}\right\} \tag{26}$$

where $\hat{\lambda}$ and ξ are arbitrary constants, and $\nu = \beta^{1/2}$. The axle therefore progresses along the track sinusoidally with frequency ν, the yaw motion leading the lateral motion by a quarter of a wavelength. In terms of real parameters, the natural frequency of the system is given by

$$\omega = V\left\{\frac{\alpha''}{br}\right\}^{1/2}. \tag{27}$$

This is a result which has been derived by many workers in the field, notably Davies (5) and Rocard (6), with the slight amendment of $\alpha'' = \alpha$: that is, they did not consider rail-head curvature.

As a means of obtaining a second approximation to the above results—and also to derive conditions for linear stability—an iteration process will be applied to the equations of motion. It will be assumed that $\ddot{\lambda} = -\beta\lambda$ and $\ddot{\theta} = -\beta\theta$. Equations (24) may then be written in matrix form as

$$\begin{bmatrix} \gamma D + (\epsilon_0 - \beta) & -\gamma \\ \gamma\sigma\beta & \gamma\sigma D - \beta \end{bmatrix} \begin{bmatrix} \lambda \\ \theta \end{bmatrix} = \begin{bmatrix} 0 \\ 0 \end{bmatrix}, \tag{28}$$

where $D = \mathrm{d}/\mathrm{d}\tau$. When the determinant of this equation is expanded, a more precise natural frequency expression is extracted as

$$\nu_1^2 = \beta\left\{1 - \frac{(\epsilon_0-\beta)}{\gamma^2\sigma}\right\}. \tag{29}$$

THE RAILWAY WHEELSET AND SUSPENSION UNIT AS A CLOSED-LOOP GUIDANCE CONTROL SYSTEM: A METHOD FOR PERFORMANCE IMPROVEMENT

By C. K. Benington*

Using a simplified mathematical model, the conventional railway wheelset and suspension unit is shown to behave as a closed-loop guidance control system. The centre-line of the track corresponds to the input, and the lateral position of the centroid of the wheelset to the output. Analysis of the system shows that, while it may be made stable at up to high speeds, the performance in the stable region is unsatisfactory in certain respects. This is attributed to the large forces of interaction between the wheels and rails at the points of contact, arising, in the case of the conventional wheelset, from creepage.

These forces may be reduced and controlled by interposing a coupling having viscous characteristics between the wheels, in place of the rigid axle. The new arrangement is shown to be much more flexible, and capable of fulfilling a wide range of performance requirements.

INTRODUCTION

RECENTLY PUBLISHED WORK (1)† indicates that the dynamic behaviour of the conventional wheelset and suspension unit is now fairly well understood. As a result, the rail vehicle designer can choose suspension parameters that will ensure stable operation over the operating speed range of a particular vehicle, at up to high speeds.

In addition to supporting the vehicle, the wheelsets act in association with the suspension and track as a closed-loop guidance control system. The performance criteria of any control system involve more than mere stability, and there are many reasons why the railway wheelset should not be exempted from more specific requirements: adequately damped transient response is important if flange and tyre wear and energy dissipation are to be kept to a minimum, and a comfortable ride is to be achieved: the bandwidth should cover only guiding frequencies, and reject 'noise' due to track irregularities.

The transfer functions of the basic conventional wheelset and suspension unit show that, as a guidance controller, it is inflexible, and that it is difficult to adapt to meet specific performance requirements.

The basic reason for this difficulty is that the tangential forces at the points of contact between wheel and rail are large compared with the forces that can be generated in practical suspension components. These forces arise from the inevitable creepage of the profiled tread of the wheel on the rail when the wheelset is disturbed from the central position.

The main purpose of this paper is the proposal and performance analysis of an unconventional wheelset unit in which the tangential forces of interaction with the rail may be brought under control at a greatly reduced level, resulting in a much more flexible system with a potentially superior performance.

To keep the analysis as straightforward as possible, a very simple linear system is used for the demonstration of comparative performance. Thus the figures produced are not for immediate application to real systems. However, the motion of the complete vehicle is obviously largely dependent on that of the wheelsets. Hence it is to be expected that the arrangement would prove equally beneficial in the context of a non-linear multi-degree-of-freedom system.

Notation

C	Couple.
c_1	Damping constant of torsional damper.
c_2	Damping constant of each fore and aft suspension unit.
$F_{x,y}$	Tangential forces of interaction at wheel-rail contact points.
$f_{x,y}$	Creepage coefficients.
$G_{A,B}(s)$	Transfer functions.

The MS. of this paper was received at the Institution on 14th April 1967 and accepted for publication on 29th November 1967. 23

* *Lecturer, Department of Mechanical Engineering, Heriot-Watt University, Edinburgh. Associate Member of the Institution.*

† *References are given in Appendix 3.*

I	Moment of inertia of wheelset about centroidal yaw axis.
J	Moment of inertia of wheelset about axis of rotation.
J_w	Moment of inertia of each wheel about axis of rotation.
K	Gain factor.
k_2	Stiffness of each fore and aft suspension unit.
M	Mass of wheelset.
$q_{1\ldots 4}$	Generalized co-ordinates.
q_ϵ	Error signal.
q_0	Output signal.
r_0	Tread radius, wheelset undisturbed.
T	Time constant.
$u_{x,y}$	Actual velocity of displacement of contact point.
V	Mean velocity of wheelset.
$v_{x,y}$	Velocity of displacement of point of contact assuming pure rolling.
α	Semi-cone angle of tread profile.
ζ	Damping ratio.
ω	Angular velocity of wheelset or wheel.

CONVENTIONAL WHEELSET AND SUSPENSION UNIT AS A CLOSED-LOOP CONTROL SYSTEM

The simplest model which, it is considered, will display the significant performance characteristics is shown in Fig. 1. It may be thought of as the wheelset at one end of a long vehicle. To limit the number of degrees of freedom to four, lateral coupling between the wheelset and the vehicle body has been assumed negligible: the body weight has been taken into account, however, in calculating the creepage coefficients. The wheel treads are assumed to have a conical profile, and the vehicle is assumed to move along parallel rails with constant velocity V.

Appropriate generalized co-ordinates with which to set up the equations of motion are shown in Fig. 2. They are q_1 the lateral displacement of the wheelset centroid from the track centre-line; q_2 the angular position of the wheelset in yaw relative to a normal to the track; q_3 the longitudinal displacement of the wheelset from the equilibrium position; and q_4 the angular position of the wheelset about the axis of rotation relative to an imaginary coincident

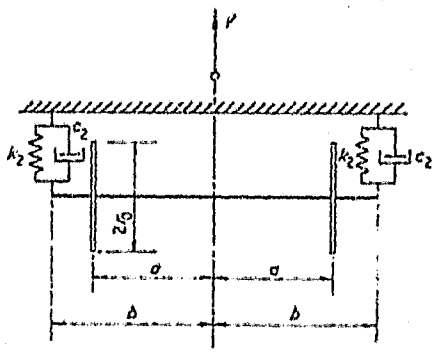

Fig. 1

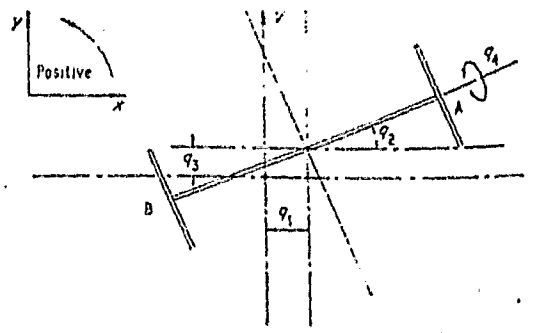

Fig. 2

wheelset rolling at the mean angular velocity, the datum being arbitrary.

The equations of motion of the wheelset, derived in Appendix 1 are:

$$I\ddot{q}_2+2\left(b^2c_2+\frac{a^2f}{V}\right)\dot{q}_2+2b^2k_2q_2-\frac{2af\alpha}{r_0}q_1=0 \quad (1)$$

$$M\ddot{q}_1+\frac{2f}{V}\dot{q}_1+2fq_2=0 \quad (2)$$

$$M\ddot{q}_3+2\left(c_2+\frac{f}{V}\right)\dot{q}_3+2k_2q_3+\frac{2fr_0}{V}\dot{q}_4=0 \quad (3)$$

$$J\ddot{q}_4+\frac{2fr_0^2}{V}\dot{q}_4-\frac{2fr_0}{V}\dot{q}_3=0 \quad (4)$$

Equations (3) and (4) are coupled, and relate to fore and aft motion only of the wheelset. When combined they yield a third-order equation which can easily be shown to be inherently stable. Fore and aft motion of the wheelset centroid is therefore uncoupled from the other motions, and is of no further interest.

Equations (1) and (2) are also coupled and define the transverse translation and yaw of the wheelset. They are therefore of direct interest.

If the unit is to be analysed as a guidance control system, the input will be the lateral position of the track centre-line relative to an arbitrary datum, and here denoted by q_i. The lateral position of the wheelset centroid relative to the same datum will be the output variable, q_0, and the error signal will be $q_1=(q_0-q_i)$ and now denoted by q_ϵ.

Equations (1) and (2) may now be written in transfer function form as

$$q_2=G_A(s)q_\epsilon \quad . \quad . \quad . \quad . \quad (5)$$

$$q_0=G_B(s)q_2 \quad . \quad . \quad . \quad . \quad (6)$$

where

$$G_A(s)=\frac{K_A}{T_A^2s^2+2\zeta_AT_As+1} \quad . \quad . \quad (7)$$

and

$$G_B(s)=\frac{-K_B}{T_Bs(T_Bs+1)} \quad . \quad . \quad . \quad (8)$$

The relationships between the gain factors and time constants and the system parameters are:

$$K_A = \frac{af\alpha}{r_0 b^2 k^2}$$

$$T_A = \sqrt{\frac{I}{2b^2 k_2}}$$

$$\zeta_A = \frac{\left(b^2 c_2 + \frac{a^2 f}{V}\right)}{\sqrt{2Ib^2 k_2}}$$

$$K_B = \frac{MV^2}{2f}$$

$$T_B = \frac{MV}{2f}$$

The system may be represented in block diagram form as shown in Fig. 3, $G_A(s)$ and $G_B(s)$ being the forward path transfer functions. Blocks A and B may be said to correspond to the controller and motor units respectively.

ANALYSIS OF PERFORMANCE OF CONVENTIONAL WHEELSET

The parameters of the standard gauge wheelset and suspension do not vary over a very wide range, and performance analysis using typical values is felt to be more fruitful than a completely general approach.

The values given below are quoted by Wickens (2) as being typical of British Rail stock:

$r_0 = 1{\cdot}75$ ft $\quad a = 2{\cdot}5$ ft $\quad b = 3{\cdot}25$ ft

$\alpha = 0{\cdot}05$ rad $\quad M = 90$ lbf s^2 ft^{-1} $\quad f = 3\times10^6$ lbf

$I = 360$ lbf ft s^2

Thus for $V = 100$ ft/s, $k_2 = 10\,000$ lbf/ft and $c_2 = 0$, for example,

$$T_A = 0{\cdot}041 \text{ s} \quad \zeta_A = 21{\cdot}5 \quad T_B = 0{\cdot}0015 \text{ s}$$

For a value of $\zeta_A \gg 1$, as in this case, the factors of the denominator of $G_A(s)$ are, to a very close approximation,

$$(1+T'_A s)(1+T''_A s)$$

where $T'_A = T_A/2\zeta_A$ and $T''_A = 2\zeta_A T_A$.

Rewriting equation (7) gives

$$G_A(s) = \frac{K_A}{(1+T'_A s)(1+T''_A s)} \quad . \quad . \quad (9)$$

Both T'_A and T_B are very small and approach zero as f approaches infinity. The transfer functions then give a purely kinematic relationship between q_c, q_2 and q_0, and the motion becomes a quasi-stable kinematic oscillation. It is apparent, therefore, that the actual motion of the wheelset is very close to the kinematic motion, and consequently will be of almost constant wavelength and very lightly damped.

The poles of the open loop transfer function, easily evaluated, are -1050, $-0{\cdot}57$, -667 and 0, corresponding to T'_A, T''_A, T_B (exponential time delay) and T_B (integrator) respectively. This array is shown on the S-plane, Fig. 4.

The simple criterion of stability

$$K_A K_B < \frac{2T_B\zeta_A}{T_A + 2T_B\zeta_A} \quad . \quad . \quad . \quad (10)$$

may be easily extracted from the characteristic equation when products of small quantities are neglected. In terms of the system parameters this criterion is

$$V < \sqrt{\frac{2ar_0 b^2 k_2}{\alpha(a^2 M + I)}} \quad . \quad . \quad . \quad (11)$$

Considering now the construction of root loci, it will be noticed that α, the tread semi-cone angle, and r_0, the mean tread radius, are the physical constants which appear only in the gain factor. Variation of gain will therefore entail a variation of, preferably, the angle α. The dominant locus breaks from the real axis at a value of approximately 0·3, and crosses the imaginary axis at $j\omega = 15{\cdot}2$ rad/s. The asymptotes are very distant, and it may be inferred that this locus is as sketched in Fig. 4. The point on the locus for $\alpha = 0{\cdot}05$ rad is shown, and this bears out the initial deduction that, while the system is stable below a critical value of gain, the damping in the st[illegible]egion is purely nominal.

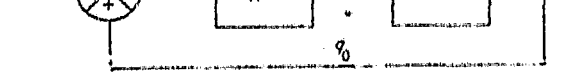

Fig. 3

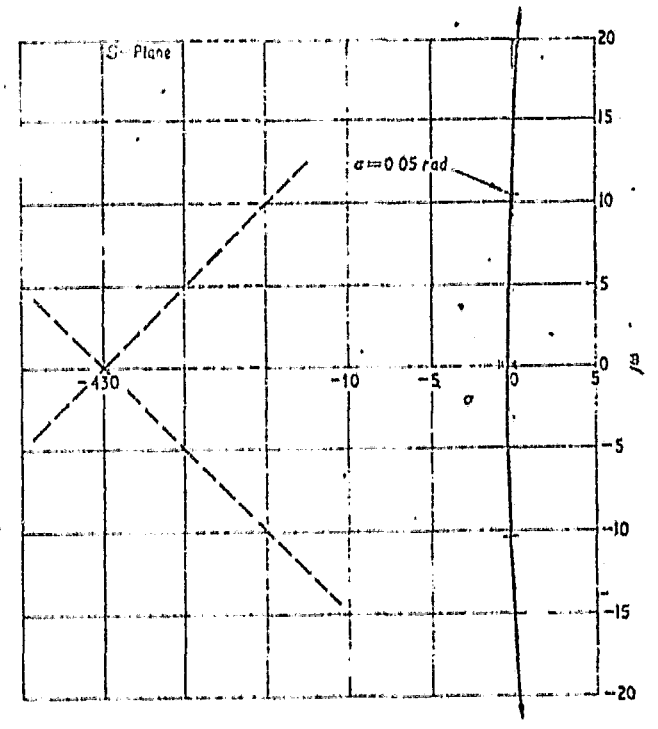

Fig. 4

The performance of this conventional system may be improved mainly by decreasing the value of T''_A. ζ_A is dominated by the creepage coefficient and cannot be decreased. (It will be noticed at this point that, while the complete influence of fore and aft dampers may not be deduced from the diagram, it is clearly not significant for practical values.) T_A may be increased by increasing the stiffness k_2, and the position of the pole corresponding to T''_A is seen to be proportional to $\sqrt{k_2}$. Once again it is clear that, while the critical gain may be significantly raised, practical limitations preclude the possibility of improving the system performance at normal values of gain.

Root loci for different values of V will display the same characteristics, and a trajectory of $\alpha = 0{\cdot}05$ will likewise be very close to the $j\omega$ axis.

While a stable transient response is a fundamental requirement curving, i.e. the ability of a wheelset to steer the vehicle round bends in the track, is important. Curving will be considered here from the purely kinematic standpoint, i.e. no account will be taken of inertia forces. If the system were linear, the curving performance would be determined by the steady state transfer between q_1 and q_2, calculable from equations (5) and (7). However, the relationship between forces due to creepage, and creepage is non-linear, the limiting value of creepage force F being given by

$$F = \mu N$$

where μ is the coefficient of friction and N the normal reaction between the wheel and rail. This limiting value of F in association with the stiffness k_2 of the longitudinal suspension units determines the minimum radius of the curve round which the wheelsets will steer a vehicle, this minimum radius being approximately proportional to the spring stiffness.

Clearly good curving performance and stability are directly conflicting requirements.

For the case under consideration, assigning to μ a value of 0·1 and assuming a vehicle wheelbase of 16 ft, the minimum radius will be about 730 ft.

ONAL APPROACH TO PERFORMANCE IMPROVEMENT

It is evident from the foregoing that, if the forces due to longitudinal creepage could be replaced by forces similar in character but greatly reduced and, if possible, variable in magnitude, improved performance could be achieved.

The longitudinal creepage forces may be eliminated by breaking the rigid coupling between the wheels, i.e. employing loose wheels. However, such a system, having zero steady state forward path transfer, would not constitute a guidance control system: but the introduction of a torsional coupling having viscous characteristics between the wheels would restore to the system on a controlled scale, forces of character similar to the longitudinal creepage forces.

ANALYSIS OF PERFORMANCE OF DAMPER-COUPLED WHEELSET

The same basic model as that shown in Fig. 1 will be used for this analysis. Breaking of the rigid torsional coupling between the wheels introduces an additional degree of freedom. The new set of generalized co-ordinates is shown in Fig. 5. q_1, q_2 and q_3 define the same rigid body displacements as before. q_4 and q_5 are incremental, describing angular displacements about the axis of rotation of each wheel relative to imaginary coincident wheels which roll without slipping, the datum in each case being arbitrary.

The equations of motion of the system, derived in Appendix 2, are:

$$I\ddot{q}_2 + 2b^2c_2\dot{q}_2 + 2b^2k_2q_2 - \frac{afr_0}{V}(\dot{q}_4 - \dot{q}_5) = 0 \quad (12)$$

$$M\ddot{q}_1 + \frac{2f}{V}\dot{q}_1 + 2fq_2 = 0 \quad (13)$$

$$M\ddot{q}_3 + 2c_2\dot{q}_3 + 2k_2q_3 - \frac{fr_0}{V}(\dot{q}_4 + \dot{q}_5) = 0 \quad (14)$$

$$\frac{J_w a}{r_0}\ddot{q}_2 + \frac{2c_l a}{r_0}\dot{q}_2 + \frac{J_w}{r_0}\ddot{q}_3 - \frac{J_u \alpha V}{r_0^2}\dot{q}_1 - \frac{2c_l \alpha V}{r_0^2}q_1 + J_w\ddot{q}_4 + \frac{fr_0^2}{V}\dot{q}_4 + c_l(\dot{q}_4 - \dot{q}_5) = 0 \quad (15)$$

$$-\frac{J_w a}{r_0}\ddot{q}_2 - \frac{2c_l a}{r_0}\dot{q}_2 + \frac{J_w}{r_0}\ddot{q}_3 + \frac{J_u \alpha V}{r_0^2}\dot{q}_1 + \frac{2c_l \alpha V}{r_0^2}q_1 + J_w\ddot{q}_5 + \frac{fr_0^2}{V}\dot{q}_5 - c_l(\dot{q}_4 - \dot{q}_5) = 0 \quad (16)$$

The term in $(\dot{q}_4 + \dot{q}_5)$ may be eliminated from equation (14) by combination with equations (15) and (16) to yield a third order equation in terms of q_3. As for the conventional wheelset, this may be shown to be inherently stable, the fore and aft motion being uncoupled from transverse and yaw oscillations.

Subtracting equation (16) from equation (15) and

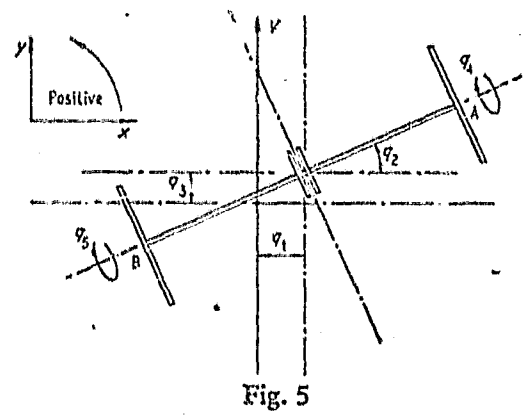

Fig. 5

flat frequency response, should permit a controlled relaxation of track standards without adversely affecting the ride.

Fringe benefits are to be expected from the virtual elimination of longitudinal creepage: these include reduced wheel tread and flange wear and energy dissipation.

The attraction of the 'ideal' system which has been proposed depends upon the feasibility of manufacturing a relatively unsophisticated and reliable torsional damper. Preliminary investigation suggests that the required performance could be obtained from a hydrostatic unit, and this possibility is currently the subject of analytical and experimental study.

ACKNOWLEDGEMENT

This work was carried out in the Department of Mechanical Engineering of the Heriot-Watt University, Edinburgh. The author wishes to express his thanks to Mr H. F. Black, a Senior Lecturer in the department, for his advice and encouragement.

APPENDIX 1

DERIVATION OF EQUATIONS OF MOTION OF CONVENTIONAL WHEELSET

The conventional wheelset consists of a pair of wheels solidly mounted on a rigid axle. The wheels are considered in this case to have conical treads.

When the motion of the wheels on the rail is other than pure rolling or slipping, the forces of interaction between the wheel and rail in the tangential plane are given by

$$F_x = -f_x\left(\frac{u_x - v_x}{v}\right) \quad . \quad . \quad . \quad . \quad (24)$$

$$F_y = -f_y\left(\frac{u_y - v_y}{v}\right) \quad . \quad . \quad . \quad . \quad (25)$$

where the subscript x indicates the lateral direction and y the longitudinal direction. The expression in brackets is defined by Carter (3) as the creepage. f is the creepage coefficient and is dependent on the normal reaction between the wheel and rail. In this case f_x is assumed equal to f_y.

For small amplitude, low-frequency oscillations such as occur in typical systems, products of small quantities may safely be neglected. Thus, at A, Fig. 2,

$$u_{A,x} = \dot{q}_1$$
$$u_{A,y} = V + a\dot{q}_2 + \dot{q}_3$$
$$v_{A,x} = -V\left(1 + \frac{\alpha}{r_0}q_1\right)q_2$$
$$v_{A,y} = \left[V\left(1 + \frac{\alpha}{r_0}q_1\right) + r_0\dot{q}_4\right]$$

and at B,

$$u_{B,x} = \dot{q}_1$$
$$u_{B,y} = V - a\dot{q}_2 + \dot{q}_3$$
$$v_{B,x} = -V\left(1 - \frac{\alpha}{r_0}q_1\right)q_3$$
$$v_{B,y} = \left[V\left(1 - \frac{\alpha}{r_0}q_1\right) + r_0\dot{q}_4\right]$$

From equations (24) and (25), the forces at the points of contact A and B, for significant values of V, and neglecting small quantities, are

$$F_{A,x} = -f\left(\frac{\dot{q}_1 + Vq_2}{V}\right)$$

$$F_{A,y} = -f\left(\frac{a\dot{q}_2 + \dot{q}_3 - \frac{V\alpha}{r_0}q_1 - r_0\dot{q}_4}{V}\right)$$

$$F_{B,x} = -f\left(\frac{\dot{q}_1 + Vq_2}{V}\right)$$

$$F_{B,y} = -f\left(\frac{-a\dot{q}_2 + \dot{q}_3 + \frac{V\alpha}{r_0}q_1 + r_0\dot{q}_4}{V}\right)$$

Thus, the generalized forces on the wheelset consist of a force

$$-2f\left(\frac{\dot{q}_1 + Vq_2}{V}\right)$$

in the lateral direction; a force

$$-2f\left(\frac{\dot{q}_3 - r_0\dot{q}_4}{V}\right)$$

in the longitudinal direction; a couple

$$2af\left(\frac{\frac{V\alpha}{r_0}q_1 - a\dot{q}_2}{V}\right)$$

in the horizontal plane, and a couple

$$2fr_0\left(\frac{\dot{q}_3 - r_0\dot{q}_4}{V}\right)$$

in the vertical plane.

The four independent equations of motion of the wheelset then are

$$I\ddot{q}_2 + 2\left(b^2c_2 + \frac{a^2f}{V}\right)\dot{q}_2 + 2b^2k_2q_2 - \frac{2af\alpha}{r_0}q_1 = 0 \quad . \quad (26)$$

$$M\ddot{q}_1 + \frac{2f}{V}\dot{q}_1 + 2fq_2 = 0 \quad . \quad (27)$$

$$M\ddot{q}_3 + 2\left(c_2 + \frac{f}{V}\right)\dot{q}_3 + 2k_2q_3 + \frac{2fr_0}{V}\dot{q}_4 = 0 \quad . \quad (28)$$

$$J\ddot{q}_4 + \frac{2fr_0^2}{V}\dot{q}_4 - \frac{2fr_0}{V}\dot{q}_3 = 0 \quad . \quad (29)$$

APPENDIX 2

DERIVATION OF EQUATIONS OF MOTION OF DAMPER-COUPLED WHEELSET

Referring to Fig. 5, and neglecting the products of small quantities

$$u_{A,x} = \dot{q}_1$$
$$u_{A,y} = V + a\dot{q}_2 + \dot{q}_3$$
$$v_{A,x} = -Vq_2$$
$$v_{A,y} = V + a\dot{q}_2 + \dot{q}_3 + r_0\dot{q}_4$$
$$u_{B,x} = \dot{q}_1$$
$$u_{B,y} = V - a\dot{q}_2 + \dot{q}_3$$
$$v_{B,x} = -Vq_2$$
$$v_{B,y} = V - a\dot{q}_2 + \dot{q}_3 + r_0\dot{q}_3$$

The forces on the wheelset in the tangential planes at the points of contact A and B may now be determined by substituting these

APPENDIX A7

ARE FINITE ANGULAR DISPLACEMENTS IN THREE-DIMENSIONAL SPACE SEQUENCE DEPENDENT

It might well be thought that too much space in this work has been devoted to defining pure rolling. To add an explanation why finite angular displacements in three-dimensional space are sequence dependent might be thought to fall into the same category; to avoid possible misunderstanding, this appendix will endeavour to show that while finite angular displacements in three-dimensional space are sequence dependent, exact coordinate transformations from one coordinate axis system to another are possible.

The initial step is to demonstrate why finite angular type displacements are sequence dependent and in order to do so, reference should be made to figures 7.1 and 7.2 where it is shown that the final position of a rectangle in an $Ox_1x_2x_3$ orthogonal coordinate axes system after two successive rotations about the Ox_2 and Ox_3 axes depends upon the sequence in which the rotations are performed. (The standard convention of the right-hand corkscrew rule of angular rotation is followed, that is, rotations viewed in the direction of the particular axis are positive if the rotation is clockwise.) Since rotations of 90° would merely rotate the coordinate axes into identical systems, it is generally necessary for coordinate transformation to adopt the restriction that angular rotations be less than 90°. Suppose that the successive angular rotations are ψ and θ so that the $Ox_1x_2x_3$ coordinate axes system is rotated into the $On_1n_2n_3$ system and then into the $O\varepsilon_1\varepsilon_2\varepsilon_3$ axes system, where ψ and θ are less

than 90°. In figure 7.3, the rotation sequence is first about the Ox_2 axis and then about the $O\eta_1$ axis while in figure 7.4 the reverse sequence is followed. Such figures are difficult to draw (and to interpret) in that in attempting to depict in two dimensions an event which takes place in three-dimensional space, it is not always easy to envisage how this occurs. Nevertheless, it ought to be apparent that, although the end results are different, the final configuration is always the same if a particular rotation sequence is strictly adhered to.

An alternative approach would be to use the concept of rotation matrices. As was shown in Chapter 5, the coordinates in one axis system rotated from that system into another axis system are always exactly related to the coordinates in the new system. Suppose that the following rotation matrices are defined:

$\underline{\underline{L}}_1$ = rotation matrix relating coordinates in the $O\eta_1\eta_2\eta_3$ coordinate axes system to the coordinates in the $Ox_1x_2x_3$ axes coordinate system if rotation occurs about the Ox_2 axis.

$\underline{\underline{L}}_2$ = rotation matrix relating coordinates in the $O\varepsilon_1\varepsilon_2\varepsilon_3$ coordinate axes system to the coordinates in the coordinate axes system if rotation occurs about the $O\eta_1$ axis.

$\underline{\underline{L}}_3$ = rotation matrix relating coordinates in the $O\eta_1\eta_2\eta_3$ coordinate axes system to the coordinates in the $Ox_1x_2x_3$ coordinate axes system if rotation occurs about the Ox_1 axis.

$\underline{\underline{L}}_4$ = rotation matrix relating coordinates in the $O\varepsilon_1\varepsilon_2\varepsilon_3$ coordinate axes system to the coordinates in the coordinate axes system if rotation occurs about the $O\eta_2$ axis.

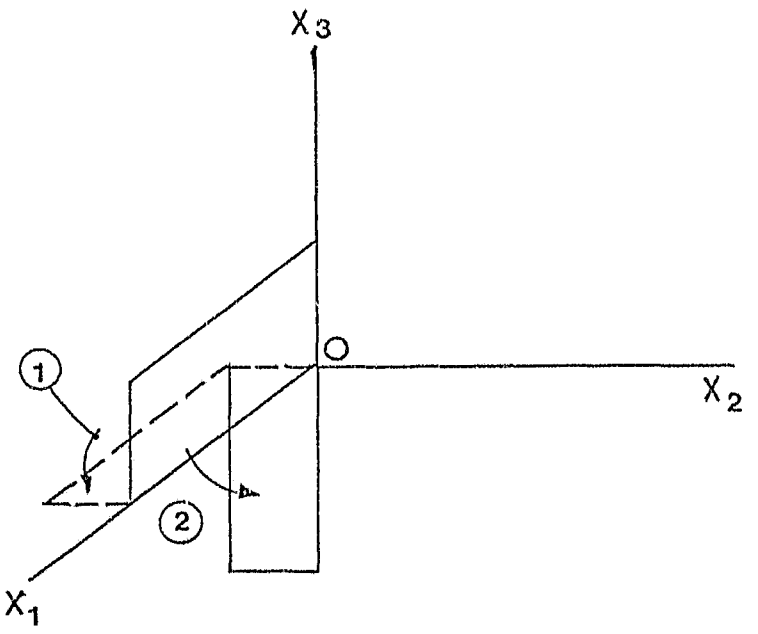

Figure 7.1: Rotation about the Ox_1 followed by rotation about the Ox_2 axis

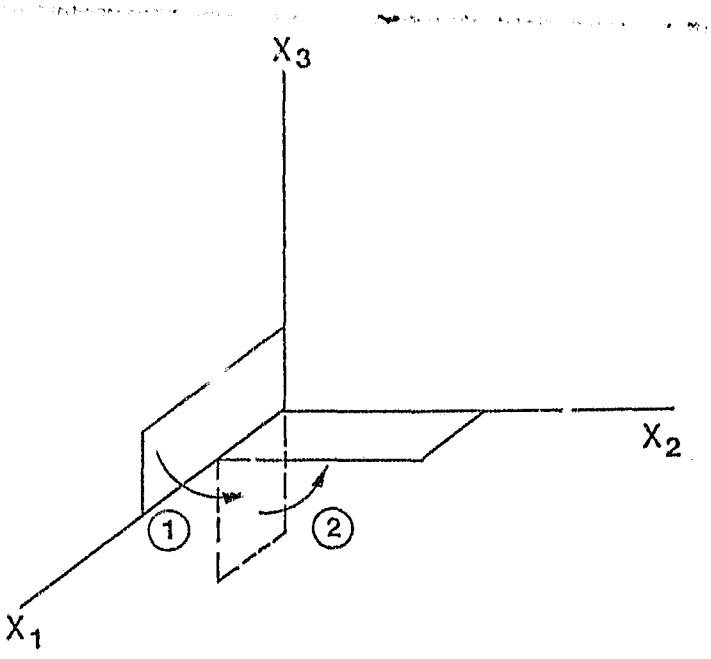

Figure 7.2: Rotation about the Ox_2 axis followed by rotation about the Ox_1 axis

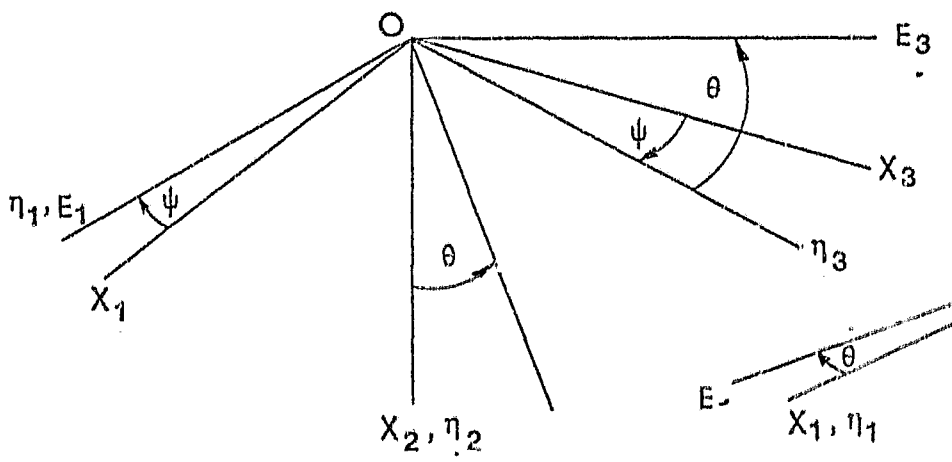

Figure 7.3: Rotation about the Ox_2 axis followed by rotation about the $O\eta_1$ axis

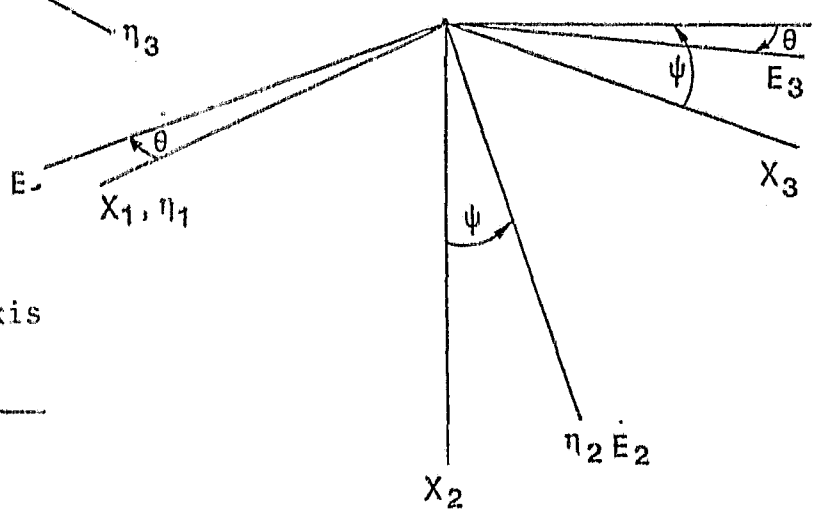

Figure 7.4: Rotation about the Ox_1 axis followed by rotation about the $O\eta_2$ axis

Suppose that $\bar{x}$ were the position vector of a given point in the $Ox_1x_2x_3$ coordinate axes space. If the $Ox_1x_2x_3$ coordinate axes system were rotated about the Ox_2 axis into the $O\eta_1\eta_2\eta_3$ coordinate axes system, the position of the point in the space under investigation does not change but the coordinates in the new coordinate axes system would be different from those in the original axes system. Suppose that this position vector is denoted by $\bar{\eta}_a$ and let the position vector after the subsequent rotation $\bar{\varepsilon}_a$. In the case where the rotations take place about the Ox_3 axis and then about the $O\eta_2$ axis, let the respective vectors be $\bar{\eta}_b$ and $\bar{\varepsilon}_b$ respectively. Then the following statements can be made:

$$\bar{\eta}_a = \bar{\bar{L}}_1\bar{x}$$

$$\bar{\varepsilon}_a = L_2\eta_a = L_2L_b\bar{x}$$

$$\bar{\eta}_b = \bar{\bar{L}}_3\bar{x}$$

$$\bar{\varepsilon}_b = \bar{\bar{L}}_4\bar{\eta}_b = \bar{\bar{L}}_4\bar{\bar{L}}_3\bar{x}$$

Since

$$\bar{\bar{L}}_2\bar{\bar{L}}_1 \neq \bar{\bar{L}}_4\bar{\bar{L}}_3$$

$$\bar{\varepsilon}_b \neq \bar{\varepsilon}_a$$

The purpose of the successive rotations is to make it possible to relate the coordinates in one system of coordinate axes with the coordinates in a different axes system. The different sequence of rotation has rotated the original set of axes into two distinct, separate coordinate axes systems, so that what has happened is that the original vector is now specified in terms of coordinates measured in these separate coordinate axes systems. Nevertheless, since both $\bar{\bar{L}}_2\bar{\bar{L}}_1$ and $\bar{\bar{L}}_4\bar{\bar{L}}_3$ are invariable matrix products under the stipulated conditions, it is possible to state, without equivocation, that the coordinate transformation from one axes system to the other system is exact providing

that the sequence of the axis systems rotations is not altered. In general, rotation matrices make it possible to convert the coordinates of any given point in the body, determined with respect to a body fixed coordinate axes system into its corresponding coordinates in the fixed axes system. The determination of the position vector of the centre of mass of the wheelpair is more complex in that the coordinates of the individual vectors in the space fixed axes system have to be evaluated before obtaining the final results.

The actual choice of the sequence in which the rotations are made might appear arbitrary but this is, in reality, not the case since a particular sequence generally facilitates the subsequent analysis. The procedure followed is that recommended by that great mathematician of the 18th century, Euler (showing that the method has a reputable ancestry). Figure 7.3 is modelled on the Euler angle procedure whereas this is not true for figure 7.4. If the dicone is made to yaw and then to tilt, the position vector of the centre of mass is obtained relatively easily as shown in the discussion in chapter 5. If, however, the dicone had been made first to tilt and then to yaw (that is, if the reverse sequence of rotations had been chosen) and if the constraint that the running surfaces were to remain in contact with the rails is observed, the resulting analysis would have been greatly complicated. The apparent freedom of choice in the sequence of the rotations is for this reason illusory.

A P P E N D I X A8

VERIFICATION OF THE VALIDITY OF THE ROOTS LISTED IN APPENDIX A8

Since some questions have been raised as to the validity of the roots derived from the characteristic equations listed in Appendix A3, the correctness of these roots have been tested as follows:

Because the frequency equation, which is of the form

$A_4 s^4 + A_3 s^3 + A_2 s^2 + A_1 s + A_0 = 0,$

is a fourth order equation, the roots of these equations must be derived by an iteration process with some cut-off point after which the iteration stops. It can then be expected that when the roots thus calculated, $x + iy$, are substituted back into the frequency equation, the resulting value of the equation would not be zero (as required theoretically) but that instead, some number $\Delta U + i\Delta V$ would be obtained. The correctness, or otherwise, of the listed roots would be judged by the magnitudes of ΔU and ΔV. In addition, if the variations in ΔU and ΔV were determined for some small change in x and y (say 1%), some measure would be afforded of the effect of the terms neglected during the iteration process.

The results of such an investigation are listed in the attached table. As the magnitudes of the coefficients A_4 to A_0 are related to the coefficient of friction, μ, and the spin speed, n, it is reasonable to expect that ΔU and ΔV would be larger as μ and n increase. Read in conjunction

with the listed values of $\Delta U/\Delta x$, $\Delta V/\Delta x$, $\Delta U/\Delta y$ and $\Delta V/\Delta y$, the data, as listed, would appear to confirm the belief that the roots shown in the thesis have been correctly derived. It should be noted that for $\mu = 0,40$ and $n = 100$, there is no higher oscillatory frequency, instead, there are two real and different roots.

VALUES OF REAL AND IMAGINARY PARTS OF FREQUENCY EQUATION = U + iV FOR EACH DERIVED ROOT x + iy, ALSO VARIATIONS IN U & V FOR 1% CHANGES IN x & y (Δx & Δy)

μ	n rad/s	ROOTS REAL (x)	ROOTS IMAG (y)	RESIDUAL VALUE * REAL (ΔU)	RESIDUAL VALUE * IMAG (ΔV)	$\frac{\Delta U}{\Delta x}$	$\frac{\Delta V}{\Delta x}$	$\frac{\Delta U}{\Delta y}$	$\frac{\Delta V}{\Delta y}$
0.05	28.46	0.181 3	3.737 6	-0.000 285 73	-0.000 982 76	- 1.832 156 99	22.959 721 43	- 22.993 374 49	- 1.861 469 03
		0.181 3	- 3.737 6	-0.000 285 73	0.000 982 76	- 1.832 156 99	- 22.959 721 43	22.993 374 49	- 1.861 469 03
		-0.686 1	9.716	-0.002 098 58	-0.002 842 80	12.509 311 47	- 58.560 611 51	60.268 527 58	12.577 106 84
		-0.686 1	- 9.716	-0.002 098 58	0.002 842 80	12.509 311 47	58.560 611 51	- 60.268 527 58	12.577 106 84
	50.00	0.263 3	3.536 5	0.000 124 97	0.000 548 79	- 2.670 560 51	25.101 803 09	- 25.156 703 75	- 2.715 181 30
		0.263 3	- 3.536 5	0.000 124 97	-0.000 548 79	- 2.670 560 51	- 25.101 803 09	25.156 703 75	- 2.715 181 30
		-1.150 1	10.213 2	0.003 505 97	-0.001 243 31	22.529 500 22	- 69.359 750 80	71.372 892 79	22.644 653 47
		-1.150 1	-10.213 2	0.003 505 97	0.001 243 31	22.529 500 22	69.359 750 80	- 71.372 892 79	22.644 653 47
	100.00	0.303 7	2.971 4	-0.000 690 62	-0.000 714 60	- 3.169 375 01	31.801 665 96	- 31.915 670 33	- 3.229 447 38
		0.303 7	- 2.971 4	-0.000 690 62	0.000 714 60	- 3.169 375 01	- 31.801 665 96	31.915 670 33	- 3.229 447 38
		-2.077 4	12.021 6	-0.352 002 08	-0.158 409 22	52.615 779 87	-118.062 545 01	121.444 678 70	52.843 113 53
		-2.077 4	-12.021 6	-0.352 002 08	0.158 409 32	52.615 779 87	118.062 545 01	-121.444 788 70	50.843 113 53
0.10	28.46	0.353 0	3.702 5	-0.000 230 99	-0.001 182 93	- 3.555 051 29	23.480 136 94	- 23.514 840 33	- 3.612 477 78
		0.353 0	- 3.702 5	-0.000 230 99	0.001 182 93	- 3.555 051 29	- 23.480 136 94	23.514 840 33	- 3.612 477 78
		-1.362 5	9.724 4	0.000 291 28	-0.000 617 36	24.784 025 76	- 57.273 662 24	59.017 648 96	24.918 381 19
		-1.362 5	- 9.724 4	0.000 291 28	0.000 617 36	24.784 025 76	57.273 662 24	- 59.017 648 96	24.918 381 19
	50.00	0.498 1	3.458 1	-0.000 123 48	0.000 841 41	- 5.002 377 30	26.128 754 54	- 26.185 296 22	- 5.087 615 81
		0.498 1	- 3.458 1	-0.000 123 48	-0.000 841 41	- 5.002 377 30	- 26.128 754 54	26.185 296 22	- 5.087 615 81
		-2.271 8	10.203 3	-0.000 697 99	0.002 161 58	44.067 371 78	- 65.069 537 55	67.165 688 87	44.293 712 67
		-2.271 8	-10.203 3	-0.000 697 99	-0.002 161 58	44.067 371 78	65.069 537 55	- 67.165 688 87	44.293 712 67
	100.00	0.569 8	2.871 5	0.001 026 91	0.001 519 30	- 5.821 903 47	33.128 319 33	- 33.240 204 47	- 5.935 671 98
		0.569 8	- 2.871 5	0.001 026 91	-0.001 519 30	- 5.821 903 47	- 33.128 319 33	33.240 204 47	- 5.935 671 98
		-4.117 2	11.776 1	-0.003 555 75	0.002 475 26	99.389 475 66	- 96.121 599 24	99.619 639 35	99.837 414 42
		-4.117 2	-11.776 1	0.003 555 75	-0.002 475 26	99.389 475 66	96.121 599 24	- 99.619 639 35	99.837 414 42
0.40	28.46	1.058 1	3.348 3	0.000 730 50	0.001 538 39	- 10.411 682 78	29.823 988 53	- 29.865 936 83	- 10.597 970 86
		1.058 1	- 3.348 3	0.000 730 50	-0.001 538 39	- 10.411 682 78	- 29.823 988 53	29.865 936 83	- 10.597 970 86
		-5.096 4	9.532 0	0.001 451 72	-0.003 864 50	85.397 840 32	- 29.442 800 82	31.509 513 07	85.891 313 23
		-5.096 4	- 9.532 0	0.001 451 72	0.003 864 50	85.397 840 32	29.442 800 82	- 31.509 513 07	85.891 313 23
	50.00	1.262 2	2.844 9	0.001 634 40	-0.001 305 51	- 11.718 800 02	35.232 511 85	- 35.294 618 49	- 11.958 745 41
		1.262 2	- 2.844 9	0.001 634 40	0.001 305 51	- 11.718 800 02	- 35.232 511 85	35.294 618 49	- 11.958 745 41
		-8.357 0	8.881 5	-0.003 775 65	-0.003 508 78	115.745 984 67	16.243 363 80	- 13.615 621 07	116.550 370 69
		-8.357 0	- 8.881 5	-0.003 775 65	0.003 508 78	115.745 984 67	- 16.243 363 80	13.615 621 07	116.550 370 69
	100.00	1.339 7	2.104 2	-0.000 361 90	-0.000 882 49	- 11.175 398 46	- 43.174 466 07	43.267 552 61	- 11.473 864 17
		1.339 7	- 2.104 2	-0.000 361 90	0.000 882 49	- 11.175 398 46	43.174 466 07	- 43.267 552 61	- 11.473 864 17

UPPER ROOTS BOTH REAL AND DIFFERENT.

* AFTER SUBSTITUTION OF ROOT IN FREQUENCY EQUATION

Author Boyd Charles Olivier
Name of thesis A Three-dimensional Analysis Of The "hunting" Of An Unflanged Railway Wheelpair In Its Motion Along A Straight Track. 1979

PUBLISHER:
University of the Witwatersrand, Johannesburg
©2013

LEGAL NOTICES:

Copyright Notice: All materials on the University of the Witwatersrand, Johannesburg Library website are protected by South African copyright law and may not be distributed, transmitted, displayed, or otherwise published in any format, without the prior written permission of the copyright owner.

Disclaimer and Terms of Use: Provided that you maintain all copyright and other notices contained therein, you may download material (one machine readable copy and one print copy per page) for your personal and/or educational non-commercial use only.

The University of the Witwatersrand, Johannesburg, is not responsible for any errors or omissions and excludes any and all liability for any errors in or omissions from the information on the Library website.